ASTROCYTIC CONTRIBUTION TO THE GLUTAMATERGIC TRANSMISSION IN SCHIZOPHRENIA

APPROVED BY SUPERVISORY COMMITTEE

Carol Tamminga, MD

Kimberly Huber, PhD

Eric Nestler, MD, PhD

Ege Kavalali, PhD

Dedicated to my mother, Constanta Stan, and to all my wonderful friends, colleagues, and mentors who supported me along the way

ASTROCYTIC CONTRIBUTION TO THE GLUTAMATERGIC TRANSMISSION IN SCHIZOPHRENIA

by

ANA DESPINA STAN

DISSERTATION

Presented to the Faculty of the Graduate School of Biomedical Sciences

The University of Texas Southwestern Medical Center at Dallas

In Partial Fulfillment of the Requirements

For the Degree of

DOCTOR OF PHILOSOPHY

The University of Texas Southwestern Medical Center at Dallas

Dallas, Texas

December, 2010

ASTROCYTIC CONTRIBUTION TO THE GLUTAMATERGIC TRANSMISSION IN SCHIZOPHRENIA

ANA DESPINA STAN, MD

The University of Texas Southwestern Medical Center at Dallas, 2008

CAROL TAMMINGA, M.D.

Schizophrenia is a chronic mental disorder encompassing an array of cognitive and behavioral manifestations. Although the disease molecular pathophysiology remains essentially unknown, evidence exists for abnormalities within all the main neurotransmitter systems and various cortical and subcortical brain structures, albeit with no unifying/overarching hypothesis connecting the existent knowledge. Moreover, no current animal model or biological construct reproduces the complexity of the disease with acceptable validity. In my work I have taken a multidisciplinary approach to study the live and postmortem human brains of people with schizophrenia, focusing specifically on the glutamatergic abnormalities in the hippocampus, one brain region repeatedly found to bear structural, molecular, and blood flow abnormalities in the disease. I have started with the *in vivo* measurement of glutamate and glutamine using magnetic resonance spectroscopy, thus getting a "high-level" sense of the glutamatergic transmission changes in the hippocampi of subjects with schizophrenia. Concretely, I have found that untreated people with schizophrenia have reduced levels of glutamate compared to their healthy counterparts, but this reduction can be partially reversed by antipsychotic medication. To allow for a more "small-scale" characterization of the glutamatergic transmission impairments, I have used postmortem brain tissue to zoom in on the glutamatergic synapse, viewed as a "tripartite synapse". Apart from the pre- and postsynaptic neurons, the third component is represented by the astrocyte, the brain glial cell that is responsible for most of the glutamate recycling and that attunes the glutamatergic synapse to the overall energetic metabolism of the brain. I have found that glutamate recycling is impaired in schizophrenia, selectively in the dentate gyrus, one of

the hippocampal subregions, and the specific abnormalities reside in the glutamate transporters, responsible clearing up synaptic glutamate.

TABLE OF CONTENTS

PRIOR PUBLICATIONS

Ana D. Stan, Subroto Ghose, Xue-Min Gao, Rosalinda C. Roberts, Kelly Lewis-Amezcua, Kimmo J. Hatanpaa, Carol A. Tamminga *Human postmortem tissue: What quality markers matter?* Brain Research 1123 (2006) 1-11

Ana D. Stan, Alan Lesselyong, Subroto Ghose *Cellular and Molecular Neuropathology of Schizophrenia* in Kalplan and Sadock's Comprehensive Textbook of Psychiatry, 9th edition, Lipincott Williams & Wilkins 2009

Carol A. Tamminga, Ana D. Stan, Anthony D Wagner *The Hippocampal Formation in Schizophrenia American Journal of Psychiatry* American Journal of Psychiatry 2010 Oct; 167 (10):1178-93

LIST OF FIGURES

LIST OF TABLES

Chapter 1

Introduction

Schizophrenia

In the absence of any diagnostic pathological or molecular features, schizophrenia is defined by the concomitant and chronic occurrence of a core set of signs and symptoms. Phenotypic analyses of patient populations have demonstrated the clustering of symptoms into three distinct categories: (1) positive symptoms, (2) negative symptoms, and (3) the cognitive impairments (Hyman and Fenton, 2003).

The positive symptom domain defines an excess or distortion of the normal mental functions and include disturbances in thought content (delusions), perception (hallucinations), speech, and behavior (disorganization) (Carpenter and Buchanan, 1994); the negative domain refers to a diminution of the normal functions, such as a limited range of emotional expression (affective flattening), social withdrawal, and anhedonia; the cognitive dysfunction reflects the disturbances of a number of cognitive functions that include, but are not limited to attention, working memory, declarative memory, and executive function (Braff, 1993; Dickinson et al., 2004; Green et al., 2000; Gur et al., 2001; Heinrichs and Zakzanis, 1998; Saykin et al., 1991). The symptom domains are not mutually exclusive; their co-occurrence in the same person is often the rule, but at certain time points one cluster may prevail (Tamminga and Holcomb, 2005).

The disease begins in adolescence or young adulthood and most typically persists for the lifetime, causing significant disturbances in many areas of psychosocial functioning. Often, the illness comes on abruptly, is episodic in nature and allows for considerable recovery between episodes. At the opposite end of the spectrum, the onset

may be insidious, with a course characterized by minimal, if any, interepisodic recovery that never comes close to the premorbid functioning (Hegarty et al., 1994; van Os and Kapur, 2009).

The phenotype heterogeneity raises interesting questions about the disease etiology and conceptualization: is schizophrenia a unique/localized lesion that manifests through a variety of signs/symptoms; if so, what are the pathogenic mechanisms that allow for such a complex expression? Or, more likely, is it a syndrome/a final dysfunctional result potentially caused by diverse insults at molecular or cellular level?

While the genetic load for the illness certainly plays a role, with a heritability of the disease of approximately 0.8, various environmental factors have been shown to be highly influential, potentially active during central nervous system (CNS) development, over a time span ranging from the *in utero* life through adolescence (Lewis and Lieberman, 2000).

Interestingly, the illness prevalence is about 1%, independent of geographical or cultural factors. The small regional differences in schizophrenia prevalence have been attributed to differential propensities in diagnosing the disease, rather than a true variation in disease distribution.

Schizophrenia and Glutamatatergic Transmission

The variability in clinical presentation and the diversity of etiological factors leaves the question of which brain regions and neurotransmitter systems could be affected in schizophrenia open; different schools of thought have advocated for various "key" brain areas predominantly affected and/or certain neurotransmitters exclusively

responsible for the disease. However, within a systems biology paradigm, schizophrenia must be a disorder of aberrant/impaired information management among multiple brain circuits and must ultimately involve several brain regions, including the prefrontal cortex (PFC), the limbic system, the thalamus and the basal ganglia (Lewis and Lieberman, 2000). The neural networks affected might be different from patient to patient, and since they are in permanent dynamic equilibrium, might be changing even in the same patient.

Dopamine over-activity in the limbic system has been intensively studied (Davis et al., 1991) and represents the domain that has contributed virtually all known therapeutics (Creese et al., 1976a, b): centrally active dopamine D2 receptor antagonists and partial agonists. Despite convincing indirect evidence supporting it (Abi-Dargham et al., 2000; Seeman and Kapur, 2000), ie, the direct correlation between clinical potency and D2 binding affinity of antipsychotic drugs (Creese et al., 1976a; Seeman et al., 1975) and the ability of indirect dopamine agonists to induce positive symptoms, dopamine dysregulation has been difficult to prove in clinical studies and explains merely a facet of the disease.

Glutamate is the other molecular target implicated by *in vivo* pharmacological data and postmortem chemistry (Carlsson et al., 2001; Coyle, 1996; Tamminga, 1998). The first clues emerged in the early 1950s from observing the actions of phencyclidine (PCP), a drug of abuse that causes symptoms indistinguishable from schizophrenia (Luby et al., 1959). The controlled studies performed in the late 1980s and early 1990s with ketamine (Krystal et al., 1994; Lahti et al., 1995b), a PCP congener, strengthened the association between this class of drugs and psychosis. Ketamine is able to produce schizophrenia-like symptoms in normal volunteers and schizophrenia volunteers in a

dose-dependent fashion (Krystal et al., 1994; Lahti et al., 2001). Interestingly, in subjects with the disease, the psychotic flare induced by ketamine displays exactly the same symptoms that the person had experienced before. In other words, ketamine activates the subject's own schizophrenia circuits (Lahti et al., 1995a; Lahti et al., 1995b).

Ketamine and PCP act as noncompetitive antagonists at the NMDA glutamate receptor (Javitt and Zukin, 1991); moreover, partial reduction of the NMDA receptor expression in mice recapitulates some symptoms of schizophrenia that could be ameliorated with antipsychotic treatment (Mohn et al., 1999). These symptoms include increased motor activity, stereotypic behavior, and poor social interaction and are amenable to be alleviated by haloperidol and clozapine (Mohn et al., 1999).

Brain regions repeatedly implicated in the pathophysiology of schizophrenia include the prefrontal cortex, hippocampus, thalamus, and the basal ganglia (Lewis and Lieberman, 2000). The major connections between these brain regions are glutamatergic, making this neurotransmitter system central to the understanding the abnormal connectivity in schizophrenia (Lewis and Moghaddam, 2006). Glutamate is the main excitatory amino acid neurotransmitter in the brain and is known to activate both ionotropic and metabotropic glutamate receptors. The ionotropic receptors, α-amino-3-hydroxyl-5-methyl-4-isoxazolepropionic acid (AMPA), kainaite (KA), and NMDA receptors, have been extensively studied at the mRNA, protein and ligand binding level in the cortex, striatum, thalamus and limbic regions in schizophrenia. The data have not been easy to integrate, but the most replicated findings are a downregulation of the NMDA NR1 subunit transcript in the medial temporal cortex (Gao et al., 2000), and thalamus. Upregulation of the NR2B subunit has been seen in the hippocampus associated with

unchanged NR2A mRNA (Gao et al., 2000). Reports showing a hypoactive NMDA receptor are supported by further studies showing reduced expression of the protein complexes which mediate their downstream signaling, such as PSD-95, neurofilament light, and SAP102 in the prefrontal cortex.

NMDA receptor abnormalities in schizophrenia have led to an interest in N-acetylaspartylglutamate (NAAG), an endogenous neurotransmitter in the human brain that is weak agonist at the NMDA receptor and a potent agonist at the mGluR3 receptor. Changes have been found in NAAG levels and its metabolic enzyme, glutamate carboxypeptidase II (GCPII) in the prefrontal cortex and hippocampus in schizophrenia (Ghose et al., 2009). Additionally, GCP II inhibitors have recently been shown to reverse effects of PCP in an animal model. It is believed that NAAG-related changes are found in schizophrenia although the precise nature is unclear.

Taken together, these data suggest that a reduction of NMDA mediated glutamatergic transmission can generate psychotic (and perhaps other related) symptoms in schizophrenia. Because of the complexity of the glutamate synapse, there are many potential sources for such a reduction. They will be examined in more detail in the next section, with focus on the astrocytic side of the excitatory synapse.

Astrocytes

Astrocytes are glial star-shaped non-neuronal cells that are ubiquitously distributed throughout the CNS. The processes of the same astrocyte can terminate in end-feet onto blood vessels or can contact the surrounding neurons. At the vascular pole, the end feet express the glucose transporter GluT 1 and are the likely site of glucose

uptake. On the neuronal side, astrocytes enwrap the synaptic terminals, making contact with both the pre-synaptic and the postsynaptic neuron (Bonvento et al., 2002), in a structure that has been described as the tripartite synapse. In the hippocampus, 57% of the axon-spine contact surfaces are associated with a presence of an astrocyte (Ventura and Harris, 1999).

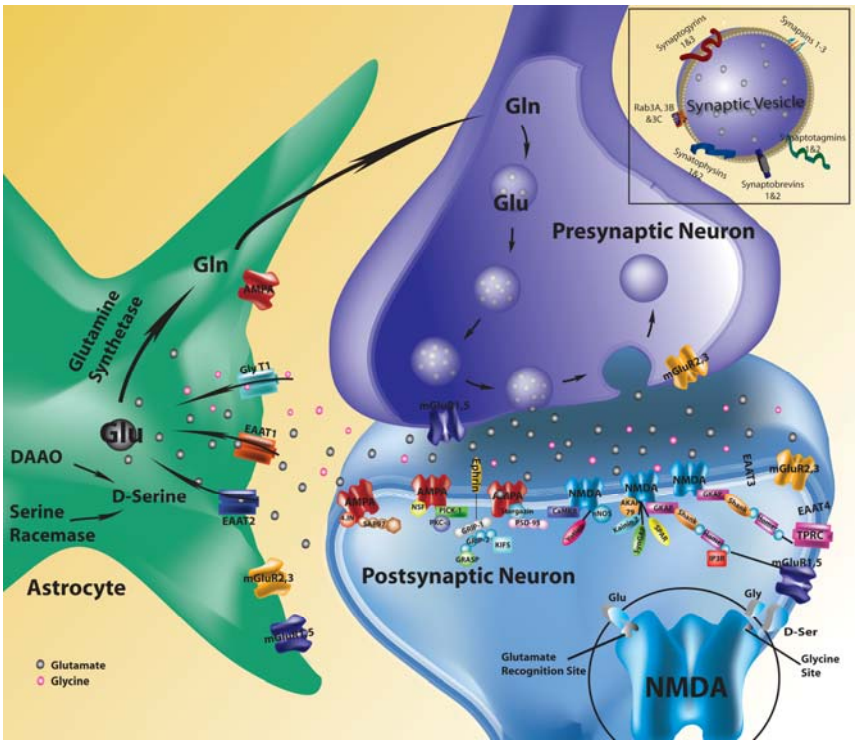

Figure 1.1. Cartoon representation of the tripartite synapse, showing the presynaptic neuron, the postsynaptic neuron, and the enwrapping astrocyte processes.

Thus, due to this structural arrangement and emerging neurochemistry, it has been proposed that the astrocytes provide a functional interface between neurons and blood vessels and act as bidirectional modulators: in one sense they supply the neurons

with metabolic constituents from the blood and in the opposite sense they convey the level of neuronal demands to the vasculature to adjust the blood flow.

Studies conducted in the early 1990s showed that in addition to their role in brain homeostasis, the astrocytes also show a form of excitability (Cornell-Bell et al., 1990). Unlike the classical electrical excitability paradigm, whereby neurons/muscle cells display a distinctive response as a result of membrane depolarization, the astrocytes respond with transmitter release to intracellular calcium fluctuations (Cornell-Bell and Finkbeiner, 1991; Dani and Smith, 1995; Verkhratsky and Kettenmann, 1996).

Cell culture and later acute brain slice experiments have demonstrated that calcium level elevation in astrocytes is triggered by neurotransmitters released by neurons, including glutamate, GABA, norepinephrine, histamine, ATP and Ach (Duffy and MacVicar, 1995; Porter and McCarthy, 1996; Shelton and McCarthy, 2000; Verkhratsky et al., 1998) that act via neurotransmitter specific receptors located on the astrocyte membrane (Fam et al., 2000; Shelton and McCarthy, 1999). More than that, an intracellular calcium increase event generated in one cell can propagate to the neighboring cells at a speed of micrometres per second through the gap junctions between the astrocytes, thus providing the basis for a circuit-like communication (Charles et al., 1991; Cornell-Bell et al., 1990; Hassinger et al., 1996; Innocenti et al., 2000; Parri et al., 2001).

Gliotransmitters released by the astrocytes include glutamate, D-serine and ATP and it has been postulated that they might modulate the strength of the synapses by activating receptors in neurons (Angulo et al., 2004; Araque et al., 1998; Fellin et al., 2004; Hamilton and Attwell, 2010; Parri et al., 2001). As astrocytes have processes that

can contact thousands of synapses simultaneously, the release of gliotransmitters contributes to the synchronization of neuronal firing patterns.

In addition to the mechanisms described above, the astrocytes are able to regulate the excitatory synaptic function in a closer way, by controlling several critical steps in the synthesis, release, and reuptake of neuronal glutamate. Apart from being an excitatory neurotransmitter, glutamate is a potent neurotoxin as well, so the precise regulation of its metabolism and concentration in the synapse is critical for the proper CNS function. Glutamate trafficking as a neurotransmitter is mainly accomplished through a major metabolic pathway known as the glutamate-glutamine cycle. Specifically, upon release from the presynaptic terminals and after binding to the specific receptors, glutamate is cleared from the extracellular space/synaptic cleft by excitatory amino acid transporters (EAATs) EAAT 1 and EAAT 2 that are expressed mainly on the astrocyte membrane. Once in the glial cell, glutamate is converted into glutamine by glutamine synthetase, an astrocyte-specific enzyme. To replenish the neuronal glutamate, glutamine is shuttled back to the presynaptic neuron, where it is transformed into glutamate by phosphate-activated glutaminase (PAG) and packed into synaptic vesicles that are prepared for release (Rothman et al., 2003). Although trace amounts of glutamate can be synthesized in the neurons, carbon-labeling experiments have demonstrated that the vast majority of the synaptically released glutamate is derived from the astrocytes through this cycle. In support of this statement is the absence from neurons of pyruvate carboxylase, the enzyme necessary to synthesize the glutamate carbon chain from glucose. Therefore, all glutamate released by neurons into the synapse must return as glutamine.

Although nuclear magnetic imaging studies of brain metabolism have generated data to substantiate that the glutamate-glutamine cycle is a major metabolic pathway in the brain, the proportion of energy required for its function relative to the total brain energy consumption is still a matter of controversy (Mason et al., 2003).

The dilemma arises from the fact that not all glutamate recovered by the astrocyte from the synaptic cleft enters the glutamate-glutamine cycle. Instead, part of it is degraded oxidatively to α-ketoglutarate and is captured in the TCA cycle, thus moving into the energetic pool. To counterbalance this loss, astrocytes synthesize glutamine by anaplerosis and restore the equilibrium of the neurotransmitter cycle. However, the percentage of glutamate that assumes an independent fate and how the energy generated by this glutamate is spent are still in debate (Patel et al., 2003).

Measurements of rates of neuronal glucose oxidation and rates of glutamate-glutamine cycle carried out in the anesthetized rat cortices established that there is a linear relationship with a slope of almost 1 above isoelectricity between the energetic metabolism and the glutamatergic signaling. This finding has important consequences on one's interpretation of metabolic imaging in the human brain: the metabolic and neurotransmitter glutamate pool are not functionally separated; on the contrary, glutamate-glutamine cycle and the brain energetic processes are coupled, and "the total pool of tissue glutamate detected by MRS appears to be in rapid communication (timescale of seconds to minutes)", indicating that the measurement of total glutamate in a volume unit offers a good estimation of the neurotransmission (Patel et al., 2003; Rothman et al., 2003).

Therefore, spatially localized MRS can offer specific data to characterize neurotransmission in a certain brain region.

The Hippocampus in Schizophrenia

Although the hippocampus is clearly not the only region to show abnormal characteristics in schizophrenia, it is reliably affected. Moreover, certain normal human memory behaviors mediated by hippocampus are those behaviors affected in the illness (Stevens, 1973).

MRI studies find consistent reductions in hippocampal or amygdalo - hippocampal volumes in schizophrenia that may be slightly more pronounced on the left side (Honea et al., 2005) . Meta analyses report hippocampal volume reductions of the magnitude of 4% in schizophrenia (Honea et al., 2005). Smaller hippocampal volumes have been shown to be present at the disease onset (Steen et al., 2006) and in disease-free first degree relatives (Tepest et al., 2003), arguing at least in part for an association with genetic vulnerability to schizophrenia, rather than with disease development. A question that remains to be answered pertains to the timeline of changes. While reduced hippocampal volumes can be identified at the beginning of the illness, imaging data attest to a progressive course (i.e., hippocampal volumes continue to decrease with disease advancement), apparently independently of the antipsychotic medication action (Panenka et al., 2007).

Hippocampal shape abnormalities (i.e., inward deformation of the head) have also been noted in persons with schizophrenia and their unaffected siblings (Csernansky et al., 2002). Moreover, left/right hippocampal asymmetry has been identified in

schizophrenia subjects, with a more accentuated inward depression of the surface of the left hippocampus, in concordance with the more accentuated volume deficit on the left side (Csernansky et al., 2002).

Intriguingly, stereological postmortem studies have failed to detect a difference in the hippocampal volume between patients and comparison subjects (Walker et al., 2002). If the volume decrease holds true, what causes it is still a matter of debate. The current consensus is that there are no significant differences in neuronal density in the hippocampus in schizophrenia although it remains a possibility that there are cell-type specific differences in subregions of the hippocampus, but this needs to be further investigated.

Functional imaging changes in regional blood flow (rCBF) in hippocampal regions were identified early in human imaging research of schizophrenia (Liddle et al., 1992; Nordahl et al., 1996; Tamminga et al., 1992). These early studies supported now with more recent findings, indicate that basal perfusion is elevated in the medial temporal lobe in schizophrenia, particularly in medication-free volunteers (Heckers et al., 1998; Medoff et al., 2001), and is "normalized" to some degree by antipsychotic treatment (Medoff et al., 2001). Some data suggest that this increase in regional perfusion correlates with the magnitude of psychosis (Lahti et al., 2006). This elevation in perfusion appears independent of activation paradigms.

The overall hypothesis of my work is that the astrocyte contributes to the neuropathology of schizophrenia by preserving a dysregulated glutamate – glutamine cycle. The exact source of the dysfunction may be in the glutamate uptake, glutamate

conversion, or in the modulation of the NMDAR co-agonist, and it may differ from case to case. Whatever the defect may be, it does not get compensated and it leads to reduced glutamate signaling.

.

Chapter 2

Materials and Methods

Human Postmortem Brain Tissue: Collection and Case Diagnosis.

Postmortem human brain tissue used in my studies was obtained from two brain banks: the Dallas Brain Collection (DBC; Dallas, TX) and the Maryland Brain Collection (Baltimore, MD). Both collection banks receive tissue from the local Medical Examiner's (ME) office. The DBC receives tissue from the Willed Body Program (WB) of the University of Texas Southwestern Medical Center and from its Transplant Service Center (TSC).

Whole human brains were harvested from recently deceased persons with psychiatric diagnoses and matched controls (persons with no psychiatric diagnosis and no evidence of a psychiatric diagnosis in first degree family members), after having obtained the next-of-kin (NOK) permission to collect the brain for neuroscience research.

Inclusion criteria were: 1) any psychiatric diagnosis; 2) suicide; 3) any age, gender, or race; 4) any normal case with the demographic characteristics matching a psychiatric case; 6) NOK permission for collection.

Exclusion criteria were: 1) traumatic injury to the head, destroying tissue; 2) forensic or medical issues requiring the brain for ME purposes; 3) agonal death; 4) no NOK available or NOK refusal to donate; 4) documented history of an infectious disease; 5) evidence, by history or examination, of current illicit drug use.

An emphasis has been placed on collecting high quality tissue, as reflected by the following characteristics: 1) cases with a relatively young age (approximately 20-50

years old, ie, the years of the most active illness); 2) unexpected death; 3) as few treatment years as possible; 4) no co-morbid drug abuse, excluding alcohol and nicotine; 5) low postmortem interval (< 24 hours with an average of 10-14 hours); and 6) high quality clinical diagnoses and clear treatment history.

To allow for a precise characterization of each case, medical records documenting the person's health history were gathered from all relevant institutions. A direct informant interview was conducted for each case with at least one family member or primary care person to obtain information to complete the Structured Clinical Interview for DSM IV-TR (SCID), the Diagnostic Evaluation after Death (DEAD), and a developmental history.

At least 2 research psychiatrists reviewed each case and made an independent diagnosis based on all available clinical information. Then a consensus diagnosis was developed and introduced into a data base, along with the demographic, treatment drug use history, and tissue quality information.

Human Brain Dissection

At the sites of collection, cases were kept cold (4 ^{o}C) between death and autopsy. A broad toxicological screen was performed for all common drugs of abuse and common therapeutic drugs. Approximately 500 medications are considered common therapeutic drugs, including mood stabilizers, antipsychotic, antidepressant, and antiepileptic drugs). At autopsy, the whole brain was removed, examined macroscopically, then placed on ice and transported to our laboratory, where it was dissected immediately.

The brain stem and cerebellum were first removed, taking care not to damage the paramedian structures. The cerebrum was then hemisected by a midsagittal cut through the corpus callosum. Using the lateral ventricle as a guide, the hippocampus and the entorhinal cortex were exposed and dissected by making a first cut from the inferior edge of the splenium towards the occipital cortex and a second cut just anterior to the amygdala. The hippocampus and the parahippocampal cortices were cut free, rolled out of the temporal lobe and placed into a specially designed mold. Embedding the structure with a Histomer polymer (Histotech, Frederiksberg, Denmark) helped preserve the "in situ" shape. Blocks of polymer-embedded tissue were then sliced at fixed 4 mm intervals in the coronal plane of the hippocampus. Once sliced, every odd-numbered coronal 4 mm chunk was frozen and the adjacent even-numbered chunk was fixed, to maximize measurement options on contiguous blocks. For my studies, I used the "middle" fixed and frozen coronal slices (ie, the 5^{th} and the 6^{th} coronal slices).

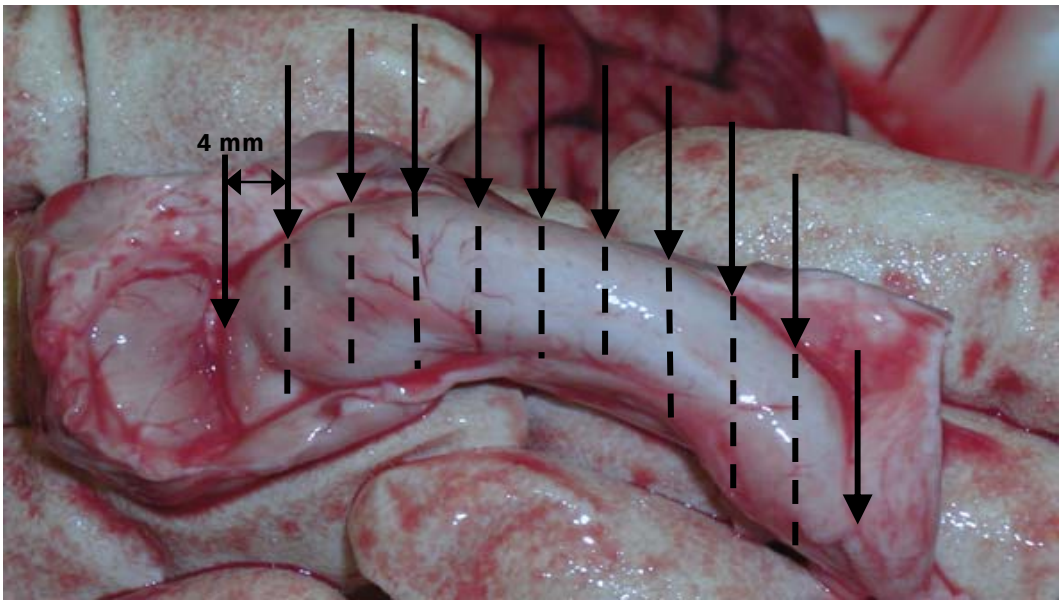

Figure 2.1. Hippocampus dissection. The structure is placed in a specially designed mold and 4 mm blocks are cut in the coronal plane along the rostro-caudal axis.

Medial Temporal Lobe (MTL) Subfield Punches

A 4 mm block of frozen MTL tissue was sectioned on the cryostat at -10 ^{o}C into 300 μm sections alternating with 20 μm sections. The 300 μm sections were placed on a glass side and stored at -80 ^{o}C for tissue punches, whereas the 20 μm sections were stained with cresyl violet.

Punches were performed on the cryostat stage at -23^{o}C. Each 300 μm section was aligned with the corresponding Nissl replicate in order to identify the hippocampal DG, CA4, CA3, CA2, and CA1 subfields. Due to the difficulty of distinguishing boundaries for CA3 and CA2 subfields, tissue from these regions was pooled. Punches were collected from the target region using a 1 mm chilled punch (Ted Pella). At least 10 punches were taken from a single region for a single sample, placed in a small centrifuge tube and put on dry ice. The material thus obtained was used for immunoblotting and quantitative PCR.

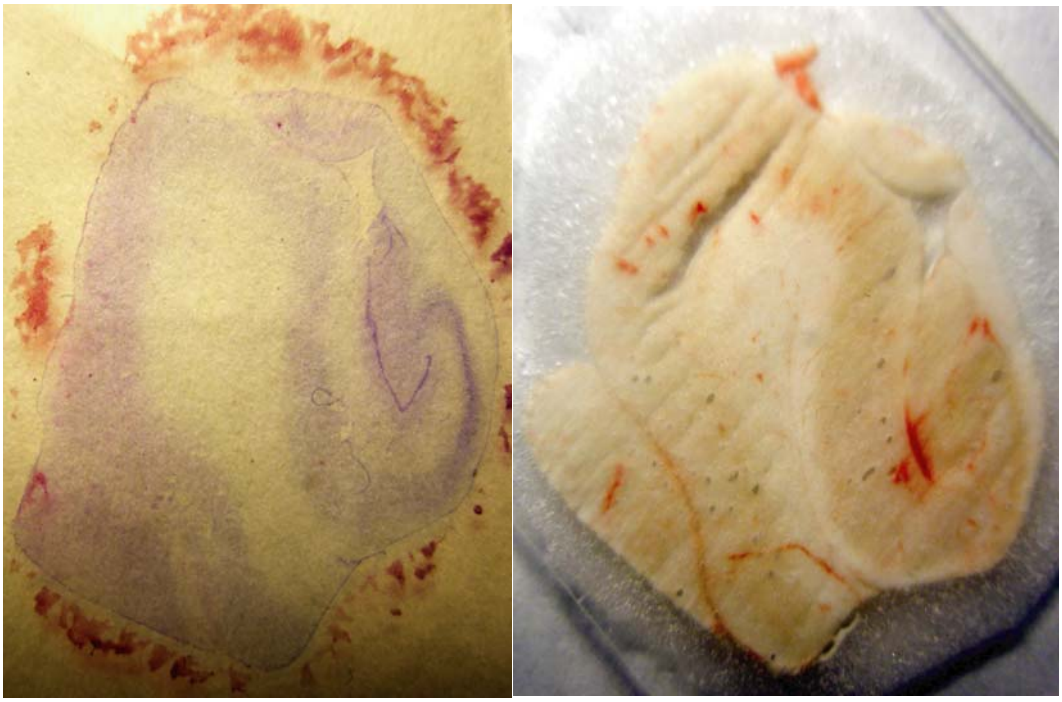

Figure 2.2. Nissl stained section aligned with the corresponding 300 μm slice of human hippocampus, showing the subfields as they appear on the slice. A 1.0 mm punch was used to gather tissue, as illustrated from DG, CA4, CA3/2, and CA1.

Quantitative PCR

Gene expression changes were determined by quantitative real-time PCR. Total RNA was isolated using Trizol reagent (Invitrogen), according to the manufacturer's protocol. Contaminating DNA was removed by DNA-ase treatment (Turbo DNA free, Ambion). RNA was converted to cDNA using Superscript III first-strand kit (Invitrogen). PCR reaction cocktails were prepared with cDNA, Power SYBR green master mix (Applied Biosystems), water and custom primers designed for each gene of interest (Operon). The PCR reactions were performed on an Applied Biosystems 7500 Real Time PCR system. Each reaction was performed in triplicate. The C_T of each gene was

normalized against that of GAPDH. All primers were first validated for linearity and specificity. The following primers have been used:

GS

Forward primer 5'- TTGAGGCACACCTGTAAACGG – 3'

Reverse primer 5'-CCCCGCAATCTTGACTCCA – 3'

EAAT1

Forward primer 5'-GAATGGCGGCGCTAGATAGTA – 3'

Reverse primer 5'-GTGCATGTTTTCCTTTGTGCC – 3'

EAAT2

Forward primer 5'-AAGTGCGAATGCCAGACAGTC – 3'

Reverse primer 5'-CAGGATGACACCAAACACCG – 3'

GlyT1

Forward primer 5'- CCTACAACCACTACCGTACCC – 3'

Reverse primer 5'- ACGGAGGACAGAGCCATGA – 3'

SR

Forward primer 5'- ATGTGTGCTCAGTATTGCATCTC – 3'

Reverse primer 5'- GCGCCCTGTTAGTTGATTCAAAA – 3'

GAPDH

Forward primer 5'- ATGGGGAAGGTGAAGGTCG – 3'

Reverse primer 5'- GGGGTCATTGATGGCAACAATA – 3'

Immunohistochemistry

In preparation for immunohistochemistry, each middle hippocampus block was fixed for 3 weeks in 4% paraformaldehyde (PF) in 0.4 M phosphate buffer (PB). PF solution was changed every 3 days. The tissue block was then cryoprotected in 10% sucrose in 0.1 M PB. The sucrose concentration was increased in a step-wise manner every other day (10%, 20%, and 30% sucrose in 0.1 M PB for a total of 6 days). Each tissue block was cut on a freezing microtome in the coronal plane at 60 μm and sections were collected in PBS containing 0.01% NaN_3.

All immunohistochemistry procedures, except for the DAB staining step, were performed using free-floating sections. All incubations took place at room temperature, unless otherwise specified. Briefly, the sections were washed in phosphate buffered saline (PBS) and endogenous peroxidase activity was quenched by 10 minute incubation in 0.3% H_2O_2 in PBS. An antigen retrieval step was completed by incubating the sections for 10 minutes in 0.01 M citric acid, pH 6.0 at 90°C. Cell membranes were then permeabilized by means of a 10 min incubation in PBS containing 0.5% Triton. To block nonspecific antibody binding, sections were incubated for 30 minutes in a solution of 4% goat serum in 0.3 % PBS Triton.

For the primary antibody step, sections were incubated overnight at 4°C in the blocking solution in which the primary antibody (Glutamine Synthetase, Chemicon) has been diluted at 1:10 000. The sections were subsequently washed in PBS and then incubated for 1 hour with goat anti-mouse IgG secondary antibodies (Vector, 1:200). Finally, sections were incubated for 1 hour with avidin-biotin HRP complex (ABC; Vectastain kit, Vector), then slide mounted and stained using DAB (Pierce). The sections

were subsequently dehydrated in increasing concentrations of alcohol and cover-slipped with DPX.

pH Determination

Approximately 150 mg of frozen cerebellar tissue was homogenized in 1.5 ml of double deionized water (pH adjusted to 7.00 with NaOH), centrifuged for 3 minutes at 8000 g at 4 degree C. Tissue from other brain areas was used, where indicated. The pH of the supernatant was measured with a pH meter (Thermo – Electron Corporation) previously calibrated with 3 standards (pH = 4.00; pH = 7.00; pH = 10.00). For each sample, determinations were made in duplicate.

Protein Analysis

For tissue quality experiments, approximately 75 mg of frozen cerebellar tissue was homogenized with a Polytron homogenizer in 1.5 ml lysis buffer (1% SDS in 1XPBS, 2µg/ml aprotinin, leupeptin and pepstatin, and 100µg/ml phenylmethane sulphonyl fluoride (PMSF)) and centrifuged for 15 minutes at 1000g at 4 degree Celsius. The protein concentration of the supernatant was determined using a BCA assay (Pierce). 30 µg of protein was mixed with 5X loading buffer (250 mM Tris HCl (pH 6.8), 10% SDS, 10%l Glycerol, 100 mM DTT and 0.2% bromphenol blue), resolved on a 12% SDS-PAGE gel, transferred to PVDF membrane (120 V, for 1.5 hours at 4 degree C), blocked in 5% milk in TBST (50 mM Tris, pH 7.4, 150 mM NaCl, 0.1% Tween-20), and incubated in primary antibody: synaptotagmin (1:1500), Rab3A (1:3000), Syntaxin1 (1:4000), Munc18 (1:1000), VCP (valosine containing protein) (1:2000). The primary

antibodies used in this study were a gift from Thomas Sudhof (UTSW). After washing with TBST, membranes were incubated in secondary antibody 125 I (1:2000) and detected using a Storm phosphor imager. All the protein levels were normalized to VCP.

For astrocyte related experiments, the immunoblotting experiments followed the same procedure as previously described, except that 5 mg of punched tissue was homogenized in 100 µl lysis buffer and 15 µg of protein was loaded per lane. The following primary antibodies were used: Glutamine Synthetase (1:10000, Chemicon), Serine Racemase (1: 1000, BD Biosciences), EAAT1 (1: 200, Santa Cruz, cat # 15316), EAAT2 (1:200, Santa Cruz, cat # 15317). After washes, membranes were incubated in secondary antibodies (Vector Laboratories 1:10000). The membranes were then incubated with ECL (Amersham) and the proteins were detected after film exposure.

RNA Analysis

Total RNA was isolated using Trizol (Invitrogen), according to the manufacturer's instructions. RNA purity was assessed using the A260/A280 ratio (A260 = absorbance at 260 nm; A280 = absorbance at 280 nm).

For tissue quality experiments, RNA integrity was further analyzed by 1.5% agarose gel electrophoresis, followed by running on an Agilent 2100 Bioanalyzer, which also automatically calculates sample concentration, 28S/18S ribosomal ratio, and the RNA Integrity Number (RIN).

Stereology

For stereological measurement of astrocyte density, the hippocampus was sliced into 4 mm-thick coronal blocks, and the middle fixed block was cut into 60 μm sections. Starting randomly from any of the first 6 sections, every other 6th section was selected and immunostained for glutamine synthetase as previously described. During the staining procedures, section thickness decreased from 60 μm to approximately 16 μm.

Each target region (DG, CA4, CA3/2, CA1) was treated as an independent area. Boundaries were delineated and regular grids of counting frames were placed onto the circled area. Pilot studies have determined a grid size of 590 X 590 μm for the DG, 750 X 750μm for the CA4, 600 X 600 μm for the CA3/2, and 1000 X 1000 μm for the CA1, with a counting box of 100 X 100 μm as optimal to sample biological variability.

The optical fractionator probe was used to sample each region in a random-systematic manner. The counting frame size on the *z* axis was set at 10 μm, leaving 3 μm guard margins on each side. The astrocytes were counted at a 100X magnification on a computerized stereology system assisted by the Stereo Investigator software (MicroBrightField).

We immunostained tissue from 21 subjects; samples from 7 subjects were not available for stereological analysis because of poor immunostaining with the GS antibody or an unavailable structure. Therefore, we analyzed 14 subjects (7 schizophrenia and 7 control subjects). Within the 14 samples, dentate gyrus and the CA4 region of 3 samples and CA1 region of 7 samples were not available because of the region was missing from the slice. Finally, we counted GS positive cell number in DG and CA4 of 11 samples (6

schizophrenia and 5 control samples in DG, and 5 schizophrenia and 6 controls in CA4), CA3/2 of 14 samples (7 schizophrenia and 7 controls) and CA1 of 7 samples (4 schizophrenia and 3 controls).

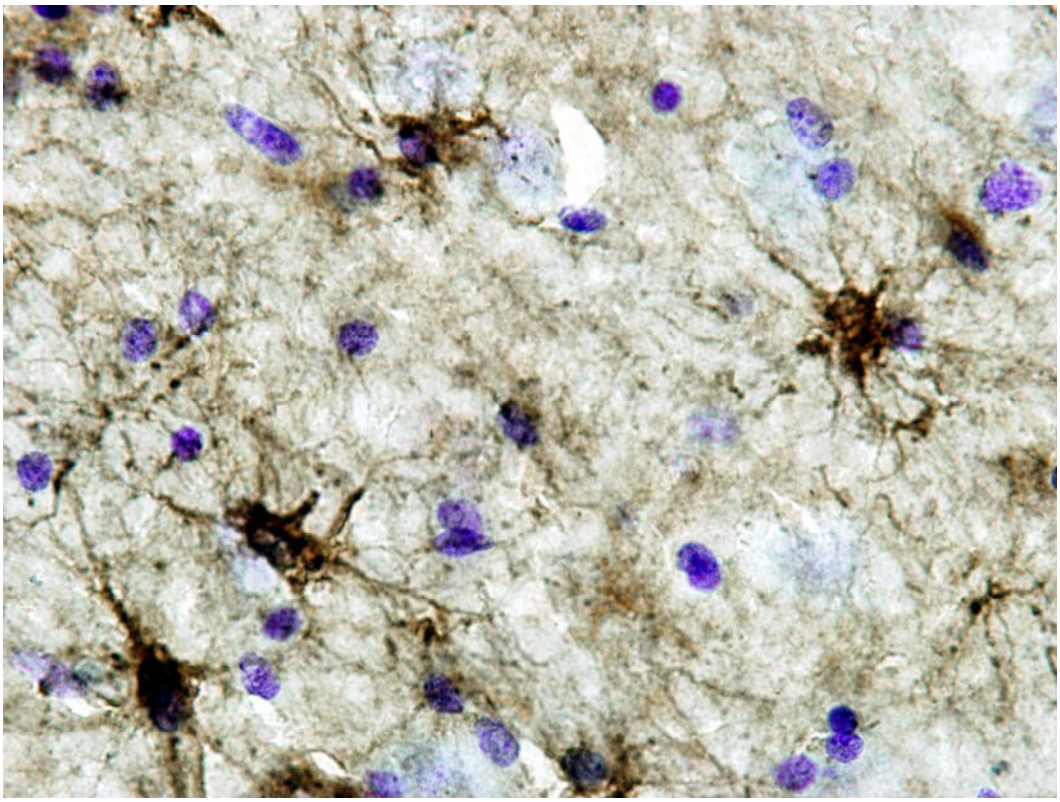

Figure 2.3 Typical glutamate staining of the astrocytes, outlining astrocytic cell body and processes.

Antipsychotic drug treatment in rats

56 rats 8 wks old were divided in 4 treatment groups (14 rats per group) that received haloperidol, olanzapine, risperidone, and water, respectively. The drugs were dissolved in double deionized drinking water and were given for a period of 20 weeks. The dosage was 1.5 mg/kg/day for haldol, 2.5mg/kg/day for olanzapine, 3.75mg/kg/day for risperidone. The animals were weighed periodically for proper dosing. One animal in

each group was sacrificed after 10 weeks to measure the blood concentration of each drug. We were targeting for values similar to the therapeutic values in humans, ie 6 – 16 ng/ml for Haloperidol, 35 – 45 ng/ml for Risperidone, and 10 – 25 ng/ml for Olanzapine. At the end of the treatment, all animals were sacrificed by decapitation. The medial temporal lobe was dissected out and homogenized with lysis buffer. The material thus obtained was used for Western blotting as described above.

Chapter 3

Quality Assessment of Postmortem Human Tissue

Introduction

Postmortem human brain tissue is increasingly being used to quantify cellular and molecular markers of CNS activity in the pursuit of understanding normal brain function and correlates of its pathological states (Casanova and Kleinman, 1990; Castensson et al., 2000; Harrison et al., 1994; Mirnics et al., 2001; Torrey et al., 2000). A key factor in conducting postmortem research is the quality of the tissue. Unlike animal tissue, whose condition at death can be controlled, human tissue can only be collected naturalistically. This introduces potential confounds, based both on pre-, and postmortem conditions, that may influence the quality of tissue and its ability to yield accurate and consistent results.

While premortem factors such as particular life experiences, prescription drug regimes, smoking, or concurrent illnesses require full documentation and carefully chosen normal controls, the agonal conditions may directly influence the morphological and biochemical integrity of brain components. It has been shown that coma, hypoxia, hyperpyrexia, seizure, multiple organ failure, and alterations in acid-base balance have the ability to lower the brain pH and promote RNA degradation (Lee et al., 2005; Li et al., 2004; Preece and Cairns, 2003; Tomita et al., 2004). All pathological states listed before have in common an increase in tissue lactate and consequently a decrease in tissue pH (Hynd et al., 2003; Kingsbury et al., 1995).

Similarly, the postmortem interval (PMI), defined as the time between death and the moment when the tissue is frozen, has been traditionally considered a primary indicator of tissue quality and used as such (Barton et al., 1993; Ferrer-Alcon et al., 2003; Harrison et al., 1995; Lewis, 2002; Trotter et al., 2002).

Consistent with the classical views on postmortem tissue integrity and in an attempt to use high –quality and well characterized brain specimens, I measured tissue quality parameters in over 100 postmortem cases collected from different sources. Subsequently, I correlated them with RNA quality (as indicated by the RNA Integrity Number (RIN)) (Imbeaud et al., 2005) and with protein quality (as measured by the level of representative proteins). My results show that the most sensible indicator of tissue quality is RIN and that there is a good correlation between RIN and the pH. No correlation developed between protein levels and the aforementioned factors. Moreover, even when RNA was degraded, the protein levels remained stable. However, these correlations did not prove true under all circumstances (e.g., thawed tissue, surgical tissue), that yielded unexpected quality indicators. These data also suggest that cases whose source was a Medical Examiner's office represent high tissue quality.

Results

Postmortem tissue characteristics by diagnosis and tissue source

I analyzed tissue samples taken from 114 individuals aged 15 years to 90 years, with the mean age of 45.3 ± 17.9 years. The tissue came from two locations (Dallas, Texas and Baltimore, Maryland) and from three sources: Medical Examiner's Office (ME), Transplant Service Center (TSC), and Willed Body Program (WB). Neither Dallas nor Baltimore collections contained low quality tissue because of strict preexisting inclusion criteria.

The demographic characteristics of the cases and parameters used to assess case tissue quality are detailed by psychiatric diagnosis in **Table 3.1**. The age range for each diagnostic group is: 16–77 years for normal controls (NL), 22–81 years for schizophrenia (SZ), 16–68 years for bipolar disorder (BD), 15–90 years for depression/suicide (D/S), and 17– 57 for other diagnoses (O). This range covers the active illness years for most of the diagnoses. Tissue quality measures are generally high with relatively low PMIs (< 24 h), few agonal events at death (AFS = 0 or AFS = 1), high pHs (> 6.4) and RINs (> 7). ANOVA showed no difference among groups in terms of age ($F(4,109)=1.77$, $p=0.14$), PMI ($F(4,108)=0.94$, $p=0.44$), pH ($F(4,102)=0.28$, $p=0.89$), or RIN ($F(4,101)=1.01$, $p=0.40$).

Table 3.1. Demographics and tissue quality characteristics grouped by diagnosis

Dx	No. of cases	Age	Gender		Race			PMI	AFS			pH	RIN
			M	F	C	AA	O		0	1	>1		
NL	36	49.9 ± 16.0	27	9	29	6	1	16.1 ± 6.8	27	7	1	6.6 ± 0.3	7.1 ± 2.3
SZ	38	46.9 ± 17.5	25	13	18	18	2	17.6 ± 9.4	22	6	2	6.6 ± 0.3	7.5 ± 2.0
BD	11	40.1 ± 17.2	7	4	11	0	0	20.4 ± 8.3	8	3	0	6.6 ± 0.3	7.0 ± 2.4
D/S	23	40.3 ± 20.4	16	7	23	0	0	18.9 ± 6.0	16	5	2	6.7 ± 0.2	8.1 ± 1.2
O	6	36.7 ± 17.6	4	2	4	1	1	19.4 ± 6.4	5	1	0	6.7 ± 0.4	7.0 ± 3.3

To address the question of which tissue source provides the highest quality tissue, I contrasted the characteristics of tissue from ME, TSC, and WB (**Table 3.2**). ANOVA indicated that there were age differences among locations ($F(3,110) = 7.02$, $p=0.0002$). The tissue from WB program had a significantly higher mean age as compared to DME ($p<0.001$), BME ($p=0.002$), and TSC ($p=0.0023$). While it appeared that the WB tissue had a lower mean RIN value (RIN=5.9 ± 2.9) than the other tissue sources (RIN=7.5 ± 2.1 for DME; RIN=7.5 ± 1.7 for BME; RIN=7.9 ± 2.1 for TSC), the difference was not significant.

Tissue quality measures from cases collected at both ME offices and TSC matched and were similarly good, with no differences in PMI ($F(3,109)=1.03$, $p=0.38$), pH ($F(3,108)=1.26$, $p=0.29$), or RIN ($F(3, 102)=1.94$, $p=0.13$).

Table 3.2. Demographics and tissue quality characteristics grouped by the source of the tissue

Tissue source	No of cases	Age	Gender		Race			PMI	AFS			pH	RIN
			M	F	C	AA	O		0	1	>1		
DME	43	40.5 ± 17.5	28	15	37	5	1	18.1 ± 6.3	26	15	2	6.7 ± 0.3	7.5 ± 2.1
BME	44	44.6 ± 14.5	24	10	21	13	0	16.7 ± 7.8	43	1	0	6.7 ± 0.3	7.5 ± 1.7
TSC	18	47.1 ± 19.2	12	6	15	2	1	17.4 ± 6.8	13	2	3	6.6 ± 0.3	7.9 ± 2.1
WB	9	68.2 ± 16.7	5	4	8	0	1	21.6 ± 13.6	5	4	0	6.5 ± 0.5	5.9 ± 2.9

Tissue Quality Indicators

pH levels where assessed in the whole collection and contrasted by diagnosis and by the tissue source. The average pH is not significantly different across any of the diagnostic groups (**Fig. 3.1**) or the collection sites (**Fig. 3.2**). Although the average pH appears lower for the brains collected from WB program, it is not significantly lower.

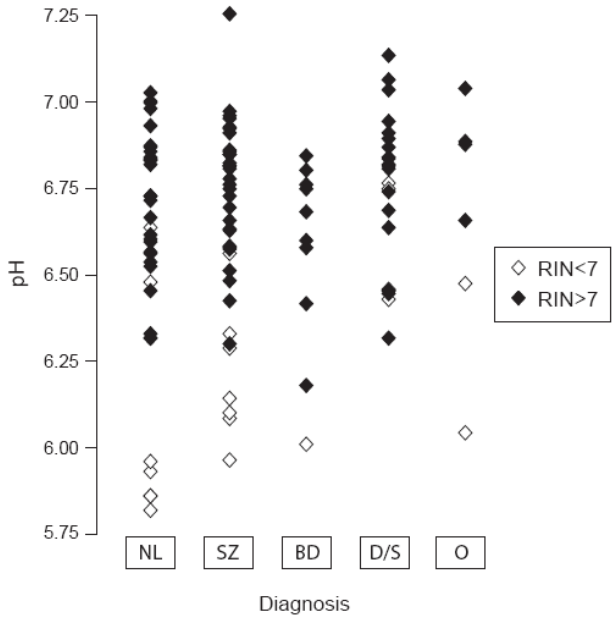

Figure 3.11. Scatterplot diagram of the pH distribution of all cases grouped by diagnosis. Within every diagnostic group, the cases with low RIN (RIN < 7) are plotted in open diamonds and the cases with high RIN (RIN > 7) are plotted in filled diamonds.

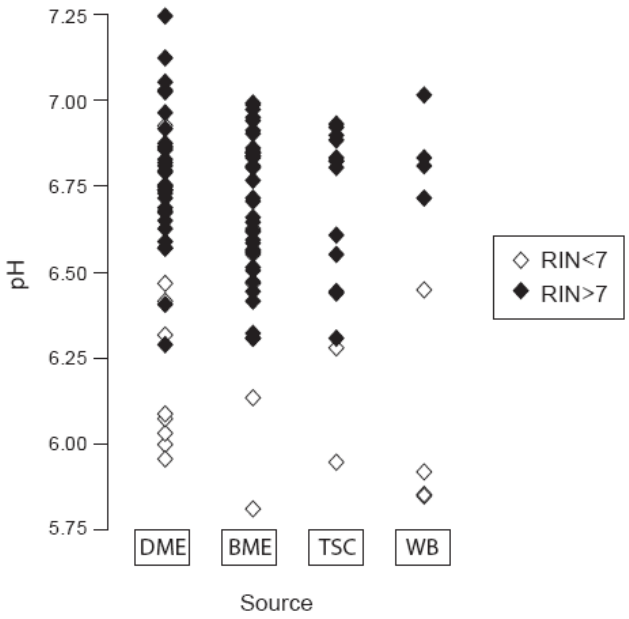

Figure 3.2. Scatterplot diagram of the pH distribution of all cases grouped by the source of tissue. Within every group, the cases with low RIN (RIN < 7) are plotted in open diamonds and the cases with high RIN (RIN > 7) are plotted in filled diamonds.

pH across different brain regions

It is possible that inner regions of the brain cool more slowly than the brain surface, therefore brain tissue in the deep areas could be exposed longer to higher temperatures, potentially affecting tissue quality. To address this question, we sampled several parts of the brain found at variable distances from the brain surface: dorsolateral prefrontal cortex (DLPFC), medial prefrontal cortex (MPFC), and the deep temporal cortex (TC).

Moreover, inside any brain region, given the higher metabolic rate of the neurons as compared to the glia, we predicted that the neurons might be more susceptible to the factors that adversely influence the tissue quality. As the gray matter (GM) is composed mostly of neuronal soma and the white matter (WM) mainly of axons and glia, a comparison between the WM and GM could provide a crude estimate of how different tissue types in the brain are conserved. We measured pH from the regions described above and found that the marker was constant across all the sampled areas and that pH in all brain regions tested is well represented by the cerebellum pH (**Table 3.3**).

Table 3.3. pH across different brain regions

Case	Index	Comparisons						Mean ± SD
	Cerebellum	DLPFC		TC		MPFC		
		WM	GM	GM	WM	GM	WM	
1	**6.1**	6.0	6.3	5.9	6.1	6.2	6.2	6.1 ± 0.1
2	**6.3**	6.5	6.5	6.5	6.5	6.5	6.5	6.5 ± 0.1
3	**6.8**	7.0	7.0	7.0	6.9	7.0	7.1	7.0 ± 0.1
4	**6.8**	6.6	6.6	6.7	6.7	6.6	6.6	6.7 ± 0.1
5	**6.8**	6.6	7.0	6.7	7.0	7.1	6.9	6.9 ± 0.2

RNA quality

Intact total RNA consists mainly of two ribosomal species: 28S and 18S. Their corresponding bands should appear crisp and well delineated on a gel electrophoresis and the 28S band should be approximately twice as bright as the 18S band. As total RNA degrades, shorter fragments progressively accumulate and the ribosomal species become less abundant; consequently, the 28S and 18S bands fade or disappear and the smaller species migrate as a smear. Illustrations of this by RNA quality are given in **Figure. 3.3.**

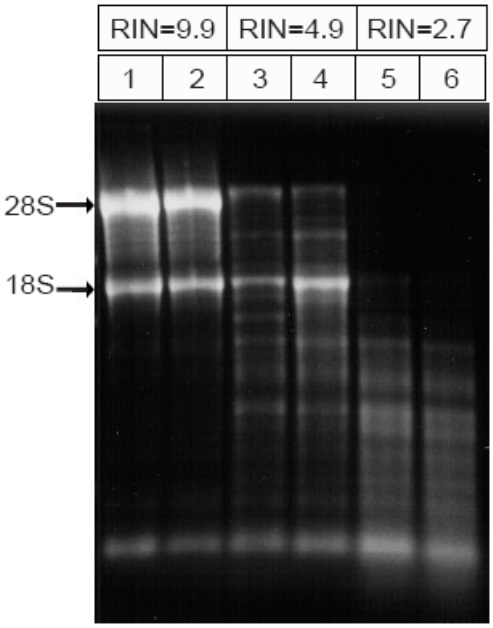

Figure 312.3. Agarose gel electrophoresis image of three representative RNA samples: intact RNA (RIN = 9.9), partially degraded RNA (RIN = 4.9), and totally degraded RNA (RIN = 2.7)

Agilent bioanalyzer

Agilent electrophoresis utilizes microcapillary electrophoresis, separating the nucleic acid molecules by size. The output is a diagram that displays fluorescence over time, with small molecules appearing at the left side of the graph. Illustrations of this by

RNA quality are in Fig. 4a (high quality), Fig. 4b (medium quality), and Fig. 4c (low quality).

With intact RNA, the baseline is flat, the two main peaks corresponding to the ribosomal species are sharp and clearly defined, and there is little noise between them (**Figure 3.4a**). With progressive degradation of the total RNA, low molecular weight material can be visualized as supplementary peaks at the left side of the curve or as a shift in the baseline, and the ribosomal peaks are lower (**Figure 3.4b**). Totally degraded RNA is made only of short fragments (**Figure.3.4c**). Classically, the 28S/18S area ratio has been used to assess the total RNA quality. The 28S:18S rRNA ratio is calculated by dividing the areas under the 18S rRNA peak into the area under the 28S rRNA peak. When RNA is intact, the ratio should be approximately 2. However, looking only at 28S/18S ratio for RNA quality does not capture the magnitude of the degradation products in the estimation of RNA quality. To solve this problem, Agilent developed an algorithm that analyzes the entire electropherogram without investigator bias and assigns a score from 1 to 10 based on the ribosomal peaks and the extent of RNA degradation products. This score is designated as RIN (RNA Integrity Number). A completely intact RNA will be attributed a RIN of 10. As more peaks different from 28S and 18S are encountered, RIN decreases accordingly to reflect the presence of the degraded material.

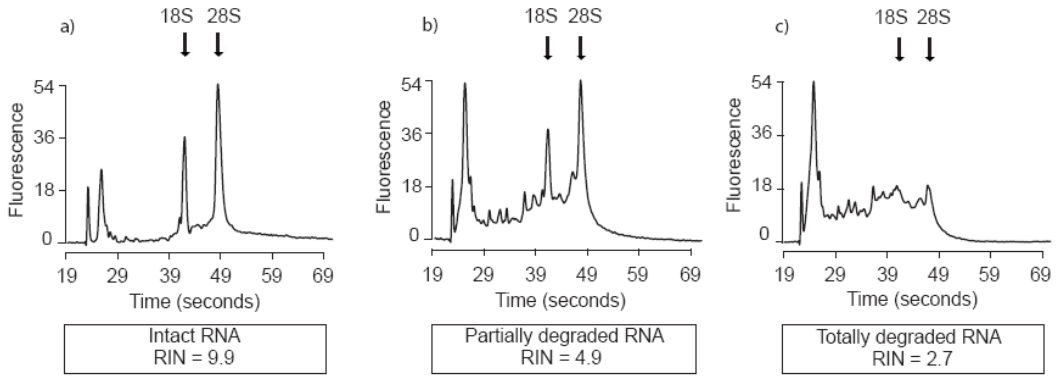

Figure 3.4. Electropherograms of three representative RNA samples: intact RNA (RIN = 9.9) (b), partially degraded RNA (RIN = 4.9) (c) and totally degraded RNA (RIN = 2.7)

Correlates of tissue quality

pH and RIN

Overall, there is a good correlation between pH and RIN (R2=0.64) (**Figure 3.5a**). RIN and pH are highly correlated in the low RIN value range (RIN<7) (R2=0.8) (**Figure 3.5b**). This correlation is not evident when looking only at higher RIN values (RIN>7) (R2=0.1), supporting the need for other tissue quality markers in addition to pH. Since most of the tissue we collected was of reasonably high quality, we may have had too few low quality cases to represent this correlation strongly.

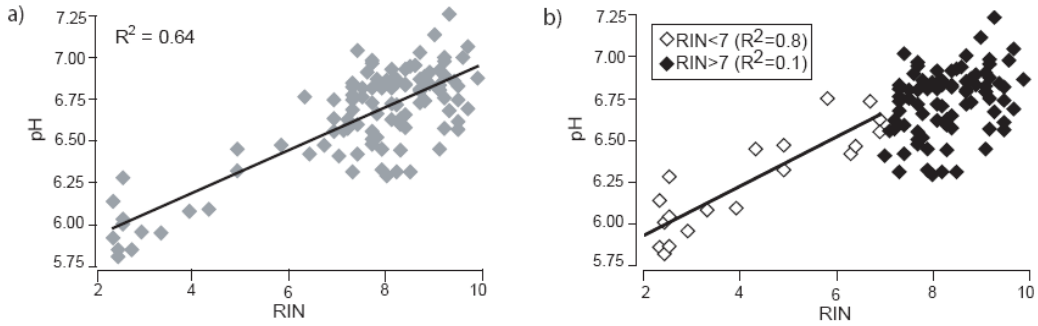

Figure 3.5. Correlations between different quality parameters: (a) pH and RIN. At low RIN values (RIN<7; white diamonds), there is a strong correlation between pH and RIN (R^2=0.8). No correlation develops at high RIN values (RIN>7; black diamonds). The correlation bar is shown only for the low RIN value range; (b) pH and RIN. There is a good overall correlation between pH ands RIN (R^2=0.6)

PMI and RIN

Postmortem interval (PMI) as used here is the interval between the time of death and the time when the brain is frozen or fixed. When the exact time of death is unknown, we use the midpoint between the last time seen alive and the time when the body is discovered. Although traditionally thought to be a good marker of high tissue quality, with a PMI range of 6 to 40 h, PMI does not correlate with the RNA quality (**Figure 3.6**). However, again, we may have lacked sufficiently long PMIs to demonstrate such a correlation.

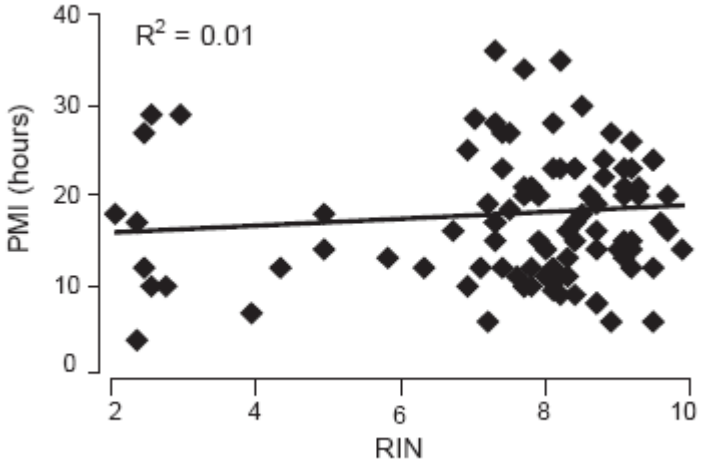

Figure 3.6. No correlation develops between PMI and RIN.

PMI and pH

Both PMI and pH have been previously used to indicate RNA quality assessment, but our data showed that there is no correlation between them, looked at independently (**Figure 3.7**). Again, a correlation might become evident in poor quality tissue.

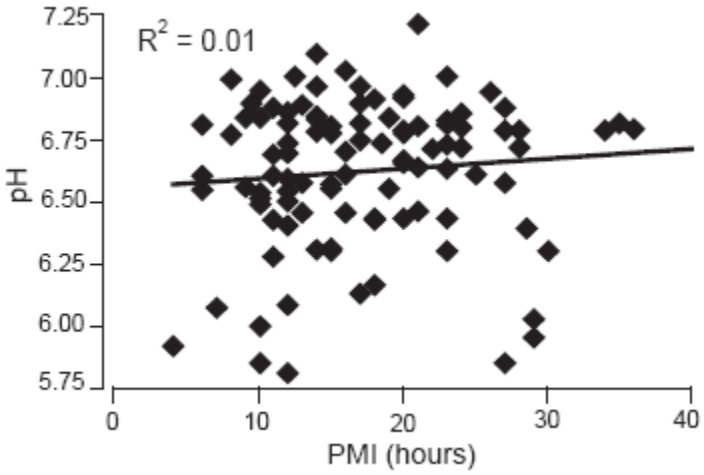

Figure 3.7. No correlation develops between PMI and pH

Protein concentration correlate

Although VCP is not widely used as a loading control, we found it to have low variability across all tissue conditions. Out of 6 protein gels, we averaged the VCP values across all lanes and normalized VCP value in every lane to the average value. The changes relative to the mean were between 0.5% and 10%, even if we loaded tissue of different PMIs, RINs and agonal conditions. Specifically, we loaded 6 protein gels: the coefficients of VCP variability for each gel were as follows: 0.07, 0.06, 0.07, 0.06, 0.05, and 0.03.

To begin to evaluate the effect of tissue quality markers on protein concentrations in the postmortem material, we measured protein concentrations illustrative proteins are stable across all of the tissue conditions available in the tissue collections we have analyzed. Neither PMI, pH, nor RIN impacts protein concentrations in the human tissue.

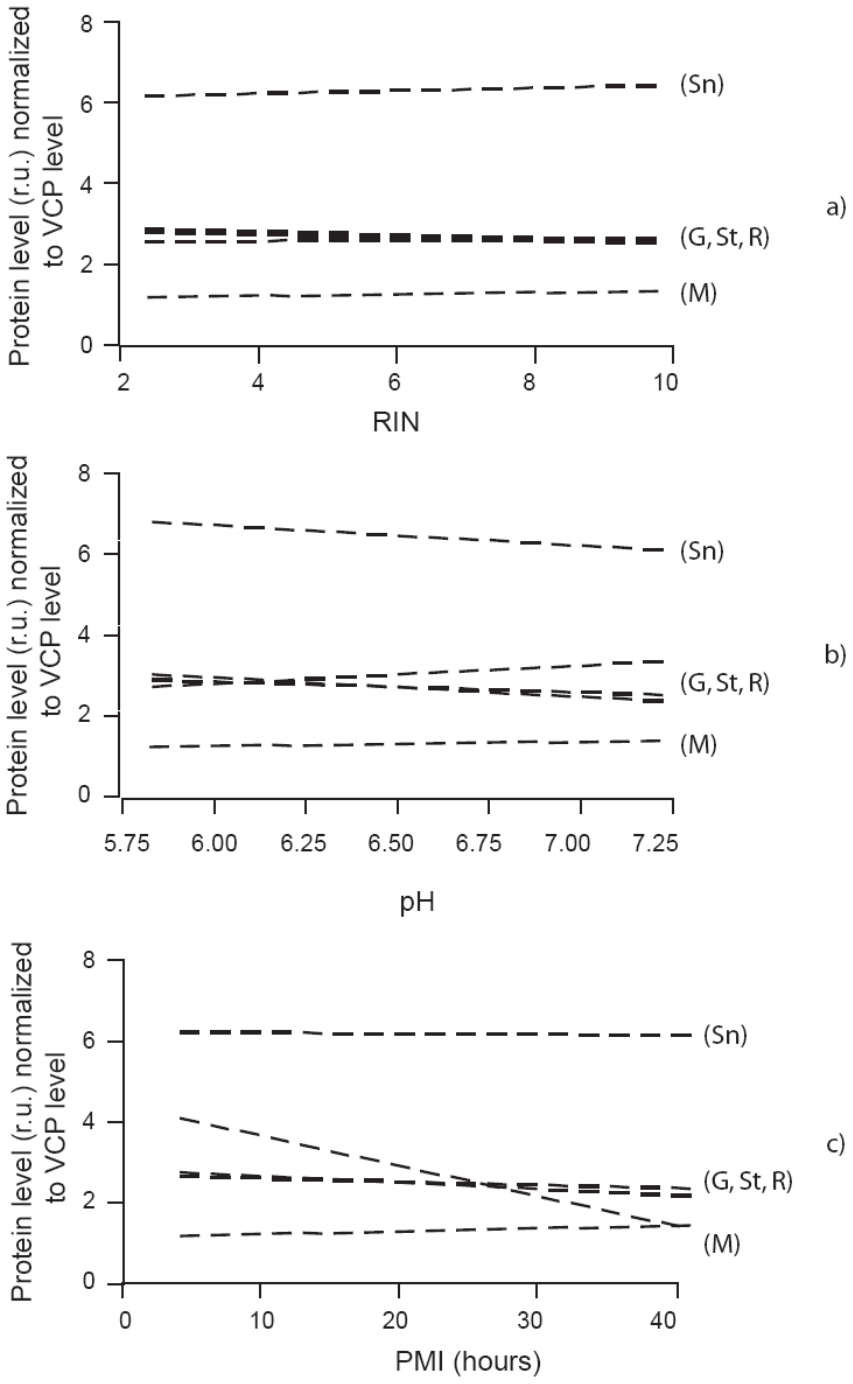

Figure 3.8. Correlation between protein level and quality parameters for five different proteins: GAPDH (G), Munc-18 (M), Syt1 (St), Rab3a (R), and Syntaxin (Sn). Only the

correlation bars are shown for the tested proteins (dotted lines). (a) protein level and RIN; (b) protein level and pH; (c) protein level and PMI. No correlation develops in any case (R^2<0.2) (see following table).

Effect of thaw

Accidentally, several pieces of cerebral tissue thawed and stayed at room temperature (in the −80 °C freezer) for up to 24 h. **Figure 3.9** illustrates the electropherograms for 3 tissue samples before and after the thaw. The pH was practically unchanged across the before and after samples. However, the RNA quality was severely degraded, as indicated by the precipitous drop of RIN and by the electrophoretic migration pattern**. Figure 3.10** shows the “before" and “after" tissue values for both pH and RIN. Although the drop in pH was significant, the value is not informative for a quality marker, given the extensive overlap between “before” and “after” values. However, nearly all RIN values in the “thawed” tissue were below 7.This example demonstrates a tissue condition where pH fails to signal the post-thaw change, whereas RIN easily discriminates the pre- and post-thaw states.

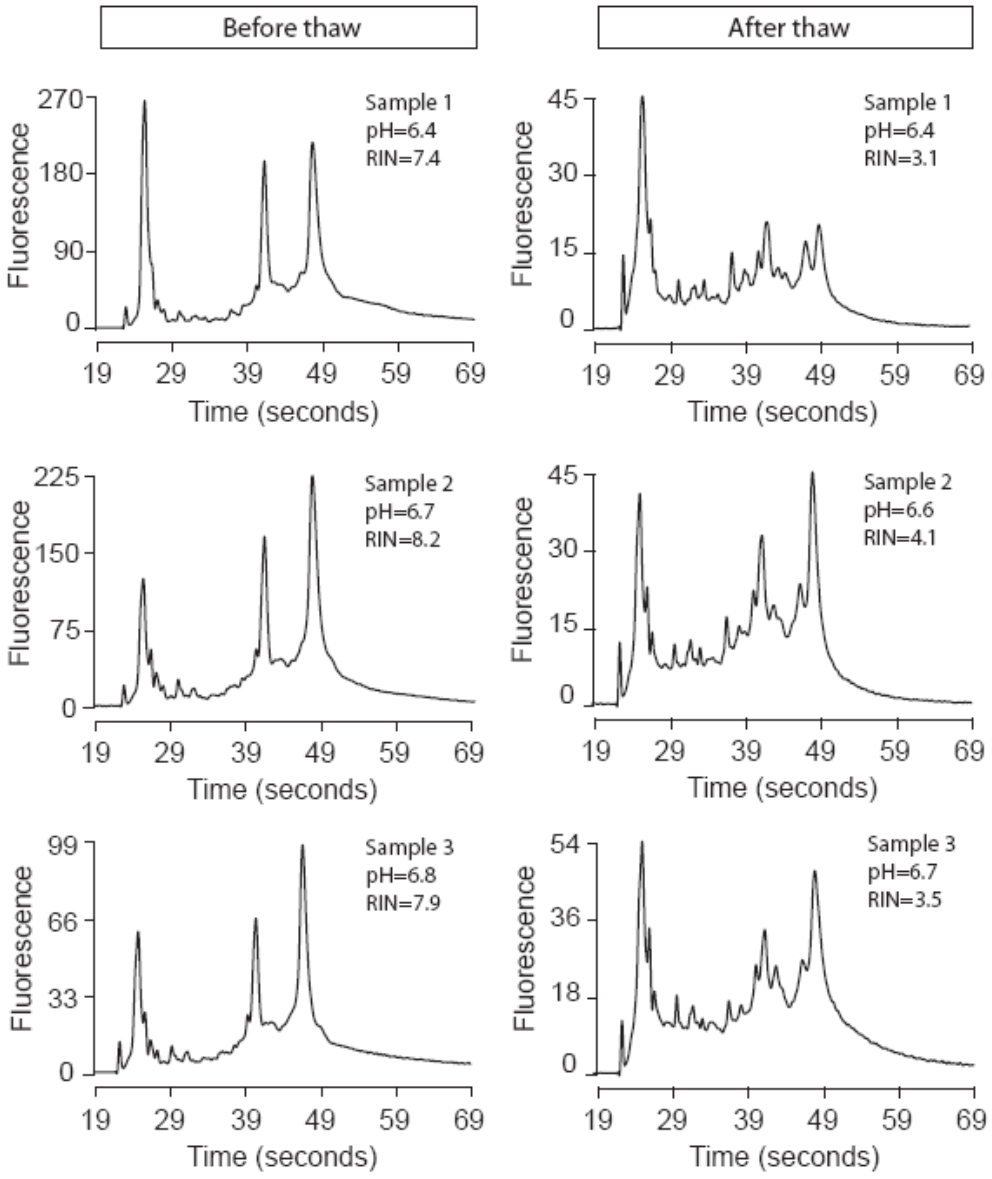

Figure 3.13. Electropherograms of three RNA samples before (left column) and after (right column) tissue thawing. The pH and RIN are written in the cassette for each condition

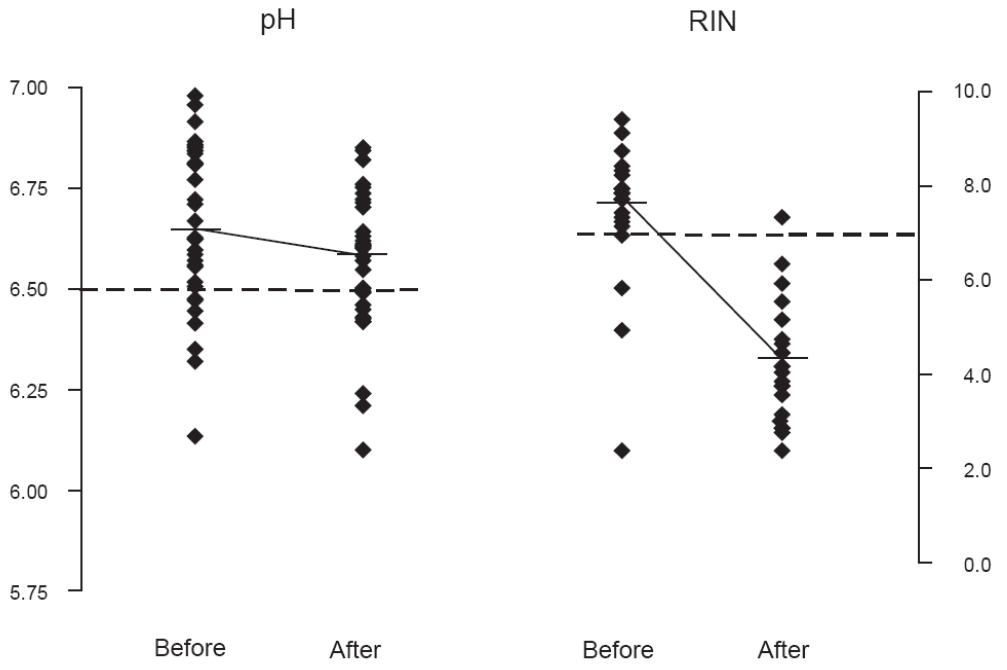

Figure 3.14. Scatterplot diagram of the pH and RIN distribution before and after the thaw. The dotted lines represent a pH value of 6.5 (our threshold for good versus low quality tissue) and a RIN value of 7 (our threshold for good versus low quality tissue). As results from the graph, most of the RIN values after the thaw are below 7

Discussion

These data show that chemical markers of tissue quality exist and suggest that they are useful in validating tissue quality. The traditional markers of tissue quality have been descriptive and included PMI, agonal condition, case age and health. In our hands, PMI was not predictive for RNA stability (within the limited quality range of our cases), confirming findings from a previous report (Trotter et al., 2002). Gradually, the field has acquired chemical markers of tissue quality, starting with pH and 28S/18S ratio, and now including direct measures of RNA quality, like RIN. The most useful human postmortem tissue quality marker in our hands is RIN. It correlates with the pH of the tissue and integrates the extent of RNA degradation with the presence of the 28S/18S peaks.

While RIN is undoubtedly a sensitive indicator of total RNA integrity and a good predictor of overall mRNA integrity,e it has been shown that under certain circumstances some specific mRNA species are preferentially degraded (Barrachina et al., 2006; Buesa et al., 2004), therefore it is advisable to verify individual mRNA integrity within an experiment. Our finding that RIN is the optimal marker for representing quality agrees with previously published studies that found RNA quality measures in assessing gene expression analysis (Colangelo et al., 2002; Jones et al., 2006; Ross et al., 1992).

pH appears to be a good marker of peri-mortem tissue quality, but does not appear to be sensitive to freezer degradation, as shown in our tissue-thaw illustration. Cerebellar tissue appears to be an adequate representative for other brain regions when testing for quality markers. Although we did not screen everywhere, we tested several representative regions from brain surface and from deep brain structures and saw pH

values correlate highly. The data suggest that measures of tissue quality from a single brain region (like cerebellum) are likely to be representative of whole brain.

Overall, we found that the cases with the best tissue quality were more likely to come from the medical examiner's office than from other collection sources. It is reasonable to assume that cases where the cause of death is fast and unexpected might demonstrate good pre-mortem conditions with low agonal stress. It must be stressed, however, that before analyzing tissue quality for the collection cases, we had already screened and excluded many ME cases who failed to meet collection criteria (e.g., drug abuse, infectious diseases, head injury) so that the cases that qualified for our collection were already pre-screened for potentially confounding conditions. Therefore, we can only claim that it is for the subset of ME cases where case confounds have already been excluded, that tissue quality is high. In contrast, the tissue collected from the WB program was from cases with advanced age and anticipated deaths, where these and other confounds might have biased tissue quality.

Somewhat unexpectedly, we showed that postmortem tissue has tissue quality markers that are at least as good as surgical biopsy tissue. Several possibilities are reasonable: still active RNA-ases in the surgical tissue, the surgical anesthesia or exposure to air while fresh. However, these results provide preliminary support for a renewed confidence in molecular measures derived from postmortem tissue (Bahn et al., 2001; Leonard et al., 1993; Preece et al., 2003).

Furthermore, the results raise the possibility that variability in molecular outcomes across CNS regions and disease groups may more likely be the result of tissue heterogeneity than postmortem degradation.

The data shown here document remarkable stability of the protein we selected in postmortem tissue. However, until further data accrue, documentation of protein stability should still be individually demonstrated for specific experiments. Nonetheless, the proteins that we selected for analysis were varied by size and tissue compartment and are, to some extent, representative. However, others have found variable protein degradation in human and animal postmortem brain using immunoblotting and immunohistochemistry techniques (Irving et al., 1997; Li et al., 1996; Liu and Brun, 1995). Even so, in most cases, protein degradation occurred at high PMIs (> 40 hours). Moreover, we do not exclude the possibility of early degradation for specific proteins.

In conclusion, we find evidence for the proposal that human high quality postmortem tissue is a generally reliable laboratory resource for exploring molecular characteristics of healthy and diseased human brain. For any RNA or protein species, its degradation characteristics in human postmortem tissue still need to be documented. Nonetheless, case screening and tissue quality assessments (including RIN) are two indispensable tools to selecting postmortem cases representative of human brain tissue.

Chapter 4

Astrocyte Regulation of Glutamatergic Transmission in the Hippocampus

As previously stated, the astrocytes regulate excitatory synaptic function by controlling several critical steps in the glutamate-glutamine cycle: 1) glutamate uptake through the specific *excitatory amino acid transporters 1 and 2 (EAATs*) located on the astrocyte membrane; 2) conversion of glutamate into glutamine by *glutamine synthetase*, an astrocyte-specific enzyme; 3) regulation of the NMDAR co-agonist Glycine and D-serine availability by the *Glycine transporter* and *serine racemase*. The molecules emphasized above will be collectively called astrocyte markers. Next section gives a more detailed description of their role, as well as regional and subcellular distribution.

1. Glutamate uptake by excitatory amino acid transporters

EAATs are membrane proteins that mediate glutamate uptake from the extracellular space into the cells, both in the peripheral tissue and in the nervous system. In fact, they can be described as "alternative access" transporters (Amara and Fontana, 2002) that can exist in two mutually exclusive working conformations: one that allows access to the transporter from the extracellular space and translocates glutamate, one H^+ ion, and three Na^+ ions into the cells; the second one provides access from the intracellular space and serves as a K^+ countertransporter.

5 members of the EAAT family have been cloned and pharmacologically characterized so far. EAAT 1 and EAAT 2 are expressed predominantly on the astrocyte processes associated with excitatory synapses (Chaudhry et al., 1995) and have been

shown to clear about 75-90% of the synaptic glutamate (Amara and Fontana, 2002; Rothstein et al., 1996). EAAT 3 – 5 are found exclusively on neuronal somas, with EAAT 3 expressed ubiquitously throughout the CNS (Danbolt, 2001), and EAAT 4 and EAAT 5 confined to the cerebellum (Furuta et al., 1997) and the retina (Arriza et al., 1997; Eliasof et al., 1998), respectively.

The two astroglial transporters are similar in their cellular localization, amino acid sequences, and affinity for glutamate; they differ by their brain regional distribution and their pharmacological properties (Arriza et al., 1994).

EAAT2 appears to be expressed more abundantly in the forebrain, where it functions as the main glutamate transporter (Milton et al., 1997; Rothstein et al., 1994). Disruption of the GLT 1 gene (homologue of EAAT2 in mouse) leads to a high probability of developing lethal spontaneous epileptic seizures and a high susceptibility to ischemic cortical injury (Tanaka et al., 1997), underscoring the critical role of EAAT 2 in clearing synaptic glutamate. Indeed, electrophysiological recordings in hippocampal slices in the homozygous mice lacking GLT 1 documented a persistent elevation in synaptic glutamate (Tanaka et al., 1997).

Unlike EAAT2, EAAT 1 is expressed more abundantly in the hindbrain (Rothstein et al., 1994); disruption if its mouse homologue gene (GLAST) yields a mild cerebellar phenotype, whereby GLAST -/- mice are able to perform simple coordination tasks, but fail at the more difficult motor ones (Watase et al., 1998).

Pharmacologically, the main difference between the astroglial transporters is that EAAT2 can be selectively modulated by kainic and dihidroxikaininc acid, or beta-lactam

antibiotics (Rothstein et al., 2005), thus raising the possibility that EAAT2 will respond differently to putative therapeutic agents.

2. Glutamate conversion into glutamine by *glutamine synthetase*

Once taken up in the astrocyte, glutamate is converted into glutamine by glutamine synthetase, whose selective expression in astrocytes has been established by ultrastructural immunocytochemistry (Martinez-Hernandez et al., 1977; Norenberg and Martinez-Hernandez, 1979); at subcellular level, glutamine synthetase can be found in the cell body and in the processes enwrapping the nerve terminals. Regarding the regional distribution, immunohistochemical studies in the rat brain showed brain wide expression of glutamine synthetase, but significant regional differences, with the highest expression in the hippocampus and the molecular layer of the cerebellar cortex (Norenberg, 1979). As pointed out in the original paper, both areas are predominantly glutamatergic.

3. Regulation of the NMDAR co-agonist Glycine and D-serine availability by the *glycine transporter (GlyT1)* and *serine racemase (SR)*

Consistent with the classical paradigm of ionotropic receptors, activation of the NMDAR results in a conformational change that allows ion exchange between extra- and intracellular space. Unlike the classical model, activation requires the binding of a co-agonist in addition to the agonist glutamate.

The two physiologic co-agonists known to date are glycine and D-serine that occupy a binding site located on the NR1 subunit and dynamically modulate NMDAR function (Kleckner and Dingledine, 1988). It is unclear, however, whether any of the 2

amino acids is the "preferred" ligand under specific conditions or in certain brain areas. Immunohistochemical studies conducted in rat brain showed that D-serine displays a higher concentration in the forebrain and a lower concentration in the caudal brain, whereas glycine immunoreactivity appears to follow an opposite pattern; nevertheless, no direct evidence exists that D-serine is the favored co-agonist in the forebrain and, for the purpose of this study, in the hippocampus.

The availability of both coagonists is subject to regulation by the neighboring astrocytes. Specifically, glycine is taken up from the synaptic cleft by Glycine transporter 1 (GlyT1), a protein expressed on the astrocyte membranes; D-serine is generated from L-serine by serine racemase, an enzyme that has both astrocytic and neuronal origin. GlyT 1 is found throughout the CNS, on the astrocyte processes, in an expression pattern that overlaps with that of the NMDA receptors. The enhanced NMDA receptor responses to GlyT 1 inhibition underscore the Glycine importance in regulating excitatory transmission. Serine racemase is the enzyme that catalyzes the conversion of L-serine in D-serine, which acts as an endogenous ligand at the NMDA receptor co-agonist site. Although initially thought to be enriched in astrocytes, serine racemase has been lately proven to be widely expressed in neurons as well. In the rat and primate brain, the regional distribution of serine racemase parallels that of D-serine, with prominent expression in the forebrain (Wolosker et al., 1999; Xia et al., 2004). SR knockout mice exhibit a 90% reduction in the content of cortex and hippocampus D-serine, underscoring the critical role of serine racemase in D-serine biosynthesis (Basu et al., 2009; Inoue et al., 2008).

Results

We have counted the astrocyte number and density and have examined the mRNA and protein levels for astrocyte related markers of glutamatergic transmission in the postmortem hippocampus derived from subjects with schizophrenia and their normal controls. The tissue used in the study was obtained from the Dallas Brain Collection. 21 cases with a diagnosis of schizophrenia and 21 normal controls were matched for age, gender, pH, RIN, and PMI.

Table 4.1 shows the demographic parameters of the schizophrenia volunteers. The sample consisted of 21 cases, 14 males and 7 females, with an average age of 47.10 ± 15.63 years. Amongst the 21 subjects, 13 were undergoing a psychotropic treatment at the time of death (on meds), 7 were not in an active pharmacological treatment (off meds), and there is no information for one subject.

A special attention was paid to the selection of high-quality postmortem tissue, with an average RIN of 8.23 ± 0.8 and an average PMI of 14.81 ± 4.16 hours.

Table 4.1. Demographic characteristics of the schizophrenia volunteers

Case no.	Sex	Age	Race	RIN	PMI	Psychotropic meds at time of death
1	M	53	C	8.3	19	on
2	M	53	C	7.7	14	not available
3	F	42	C	7.8	14	off
4	M	68	AA	8.4	17	on

5	M	33	C	8.4	20	on
6	M	52	C	9.3	21	on
7	F	43	C	6.9	11	off
8	F	85	C	8.4	9	on
9	M	26	C		24	on
10	F	73	C	4.9	14	on
11	M	41	AA	8.1	9.45	off
12	F	22	C	6.3	12	off
13	M	40	C	7	9	on
14	M	49	C	8.1	16	off
15	F	47	C	7.9	14.5	off
16	M	48	C	8.9	13.4	on
17	M	22	C	8.2	15	off
18	M	43	C	9.4	11	on
19	M	53	AA	8.6	18.3	on
20	F	71	C	8.6	17.2	on
21	M	51	C	9.1	14	on

The demographic parameters of the normal volunteers are listed in the **Table 4.2**. In summary, our sample consisted of 16 male and 5 female subjects with an average age of

47.50 ± 13.93 years. The average PMI was 16.35 ± 4.90 hours and the average RIN = 8.21 ± 1.04.

Table 4.2. Demographic characteristics of the normal volunteers

Case no.	Sex	Age	Race	RIN	PMI
1	F	56	C	6.5	16
2	M	48	C	7	14
3	M	49	AA	7.6	13
4	F	80	C	8.7	8
5	M	36	C	7.4	23
6	M	49	L	9.5	24
7	M	49	C	9.5	12
8	F	52	C	6.4	17.15
9	M	31	AA	7.5	14
10	F	73	C	5.3	18
11	M	46	C	7	24
12	M	23	AA	8	16
13	M	39	AA	8.3	22
14	M	54	C	7.6	19
15	F	41	C	8.5	15
16	M	47	C	8.9	9.37

17	M	19	C	9	20
18	M	48	C	9.5	15
19	M	60	C	8.5	20
20	M	60	C	9.8	17.1
21	M	63	AA	8.9	8.3

Rationale for subfield dissection

The hippocampal formation includes the hippocampus proper (cornu ammonis 1-3, [CA1-3], dentate gyrus [DG], and subiculum [Sub]), and the surrounding perirhinal (PRC), parahippocampal (PHC) and entorhinal (EC) cortical areas. Its component structures are arranged hierarchically and topographically (Duvernoy and Bourgouin, 1998; Insausti et al., 1998; Lavenex and Amaral, 2000). The primary projections to hippocampus come from the EC through the perforant and trisynaptic pathways; the EC in turn receives projections largely from the PRC and PHC. In particular, dense neocortical projections from multimodal association and sensory neocortex pass through PRC and PHC to EC, and then onto the hippocampus in a topographic fashion. The trisynaptic pathway is unidirectional and projects through hippocampus from EC (Layer 2) to DG, on to CA3, then to CA1. Perforant projections from EC/Layer2 also project directly to CA3, whereas EC/Layer 3 directly projects to CA1. It is believed that each anatomic region in this pathway plays a differential role in information processing, with regional processing and across-regional interactions collectively enabling the hippocampal functions. Furthermore, a discrete perturbation at any point in this

topographical, hierarchical organization may propagate within the entire network. Therefore, in order to capture the specifics of each subfield, the hippocampal tissue used in this study was dissected in the component subfields that were analyzed individually.

The results are reported separately for mRNA and protein values of glutamine synthetase (GS), serine racemase (SR), EAAT1, EAAT 2, and Glycine transporter 1 (GlyT1) in each hippocampal subdivision: dentate gyrus (DG), CA1, CA3/2, CA4.

Glutamine Synthetase (GS)

GS mRNA

There is no significant change in glutamine synthetase mRNA levels in any of the studied regions. (p = .42 DG; p = .74 CA1; p = .27 CA32; p = .35 CA4)

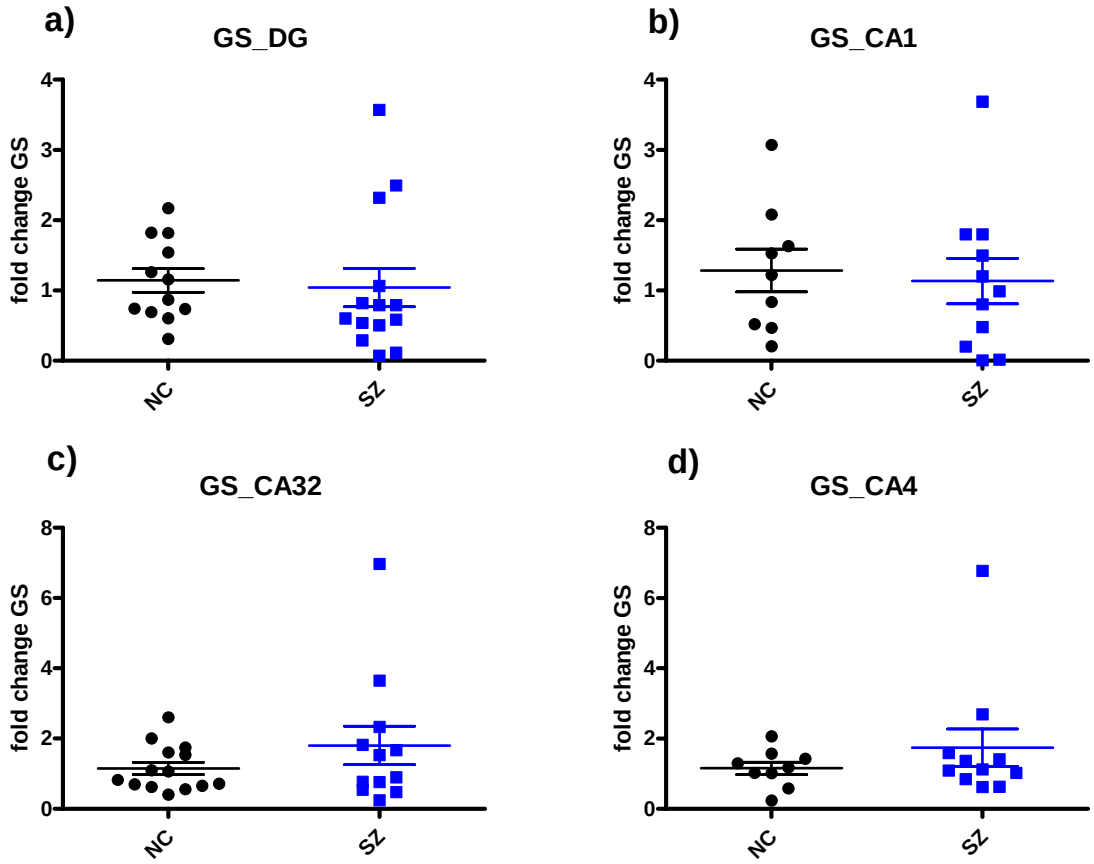

Figure 4.1. Fold changes in mRNA levels of glutamine synthetase in the DG (a), CA1 (b), CA32 (c), CA4 (d).

GS Protein

There is no significant change in glutamine synthetase protein levels in any of the studied regions. (p = .54 DG; p = .22 CA1; p = .30 CA32; p = .97 CA4)

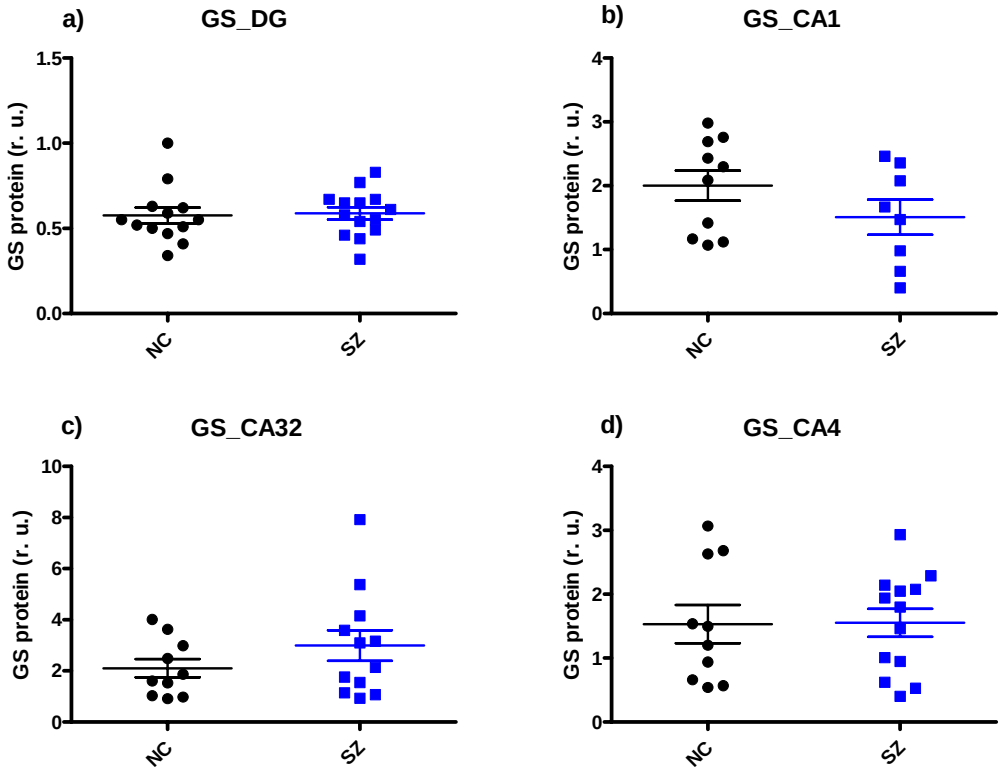

Figure 4.2. Glutamine synthetase protein levels (normalized to VCP) in the DG (a), CA1 (b), CA32(c), CA4 (d).

Serine Racemase (SR)

SR mRNA

There is no significant change in glutamine synthetase mRNA levels in any of the studied regions. (p = .73 DG; p = .55 CA1; p = .44 CA32; p = .52 CA4)

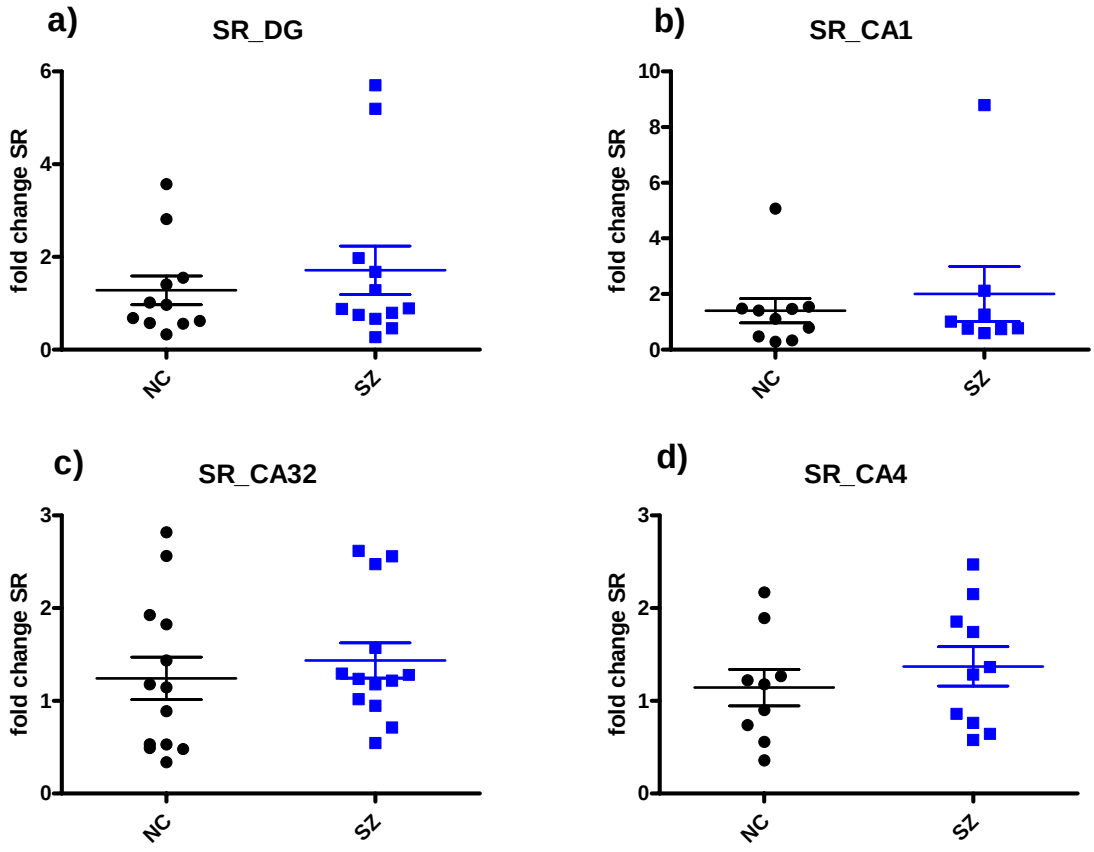

Figure 4.3. Fold changes in mRNA levels of serine racemase in the DG (a), CA1 (b), CA32 (c), CA4 (d).

SR Protein

There is no significant change in serine racemase protein levels in any of the studied regions. (p = .33 DG; p = .42 CA1; p = .11 CA32; p = .59 CA4).

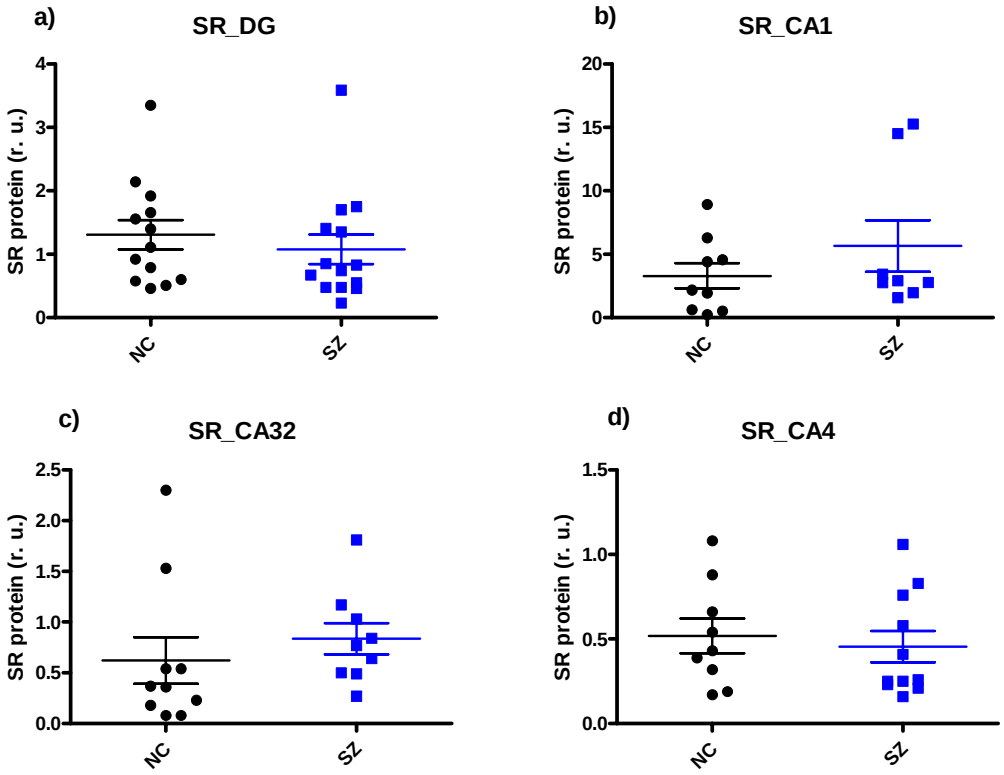

Figure 4.4. Serine racemase protein levels (normalized to VCP) in the DG (a), CA1 (b), CA 32 (c), CA4 (d).

EAAT1

EAAT1 mRNA

There is no significant change in EAAT 1 mRNA levels in any of the studied regions. (p = .37 DG; p = .34 CA1; p = .41 CA32; p = .12 CA4).

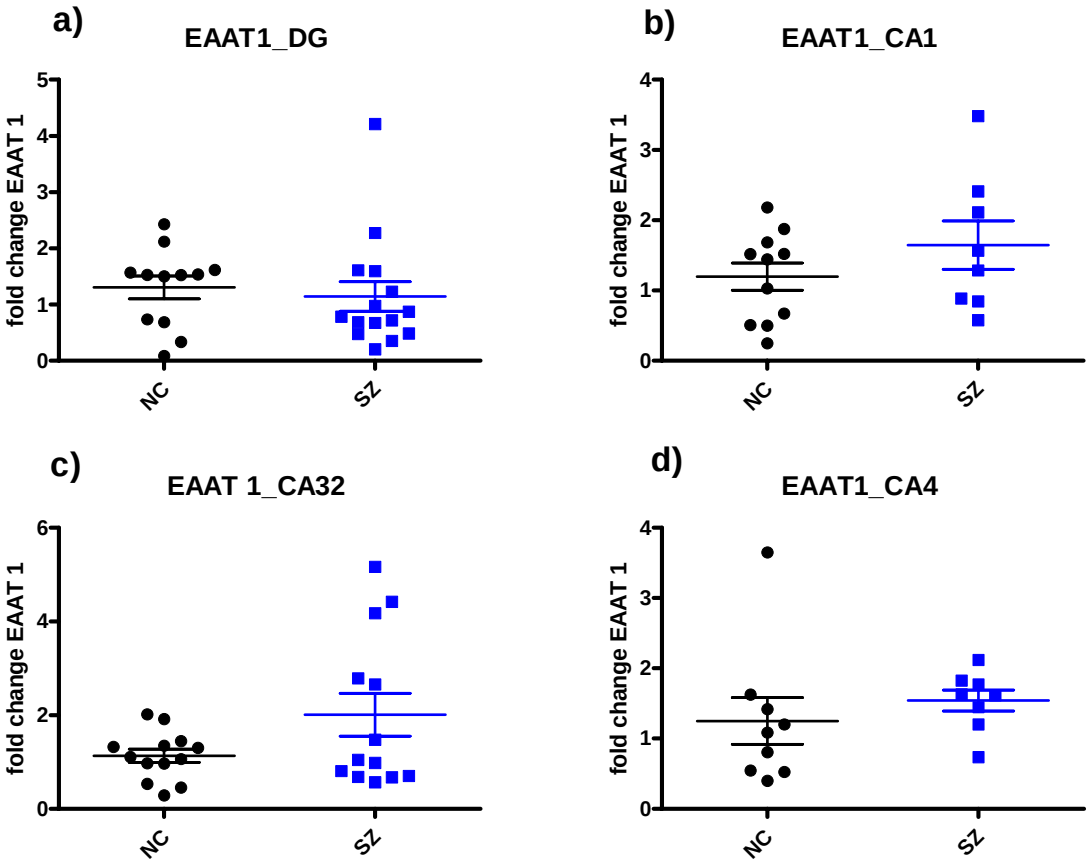

Figure 4.5. Fold changes in EAAT 1 mRNA levels in the DG (a), CA1 (b), CA32 (c), CA4 (d).

EAAT1 protein

There is a significant increase in EAAT1 protein levels in schizophrenia in the DG (p= 0.03) and no difference between the two groups in CA1 (p = 1), CA32 (p = 0.97) and CA4 (p = 0.68).

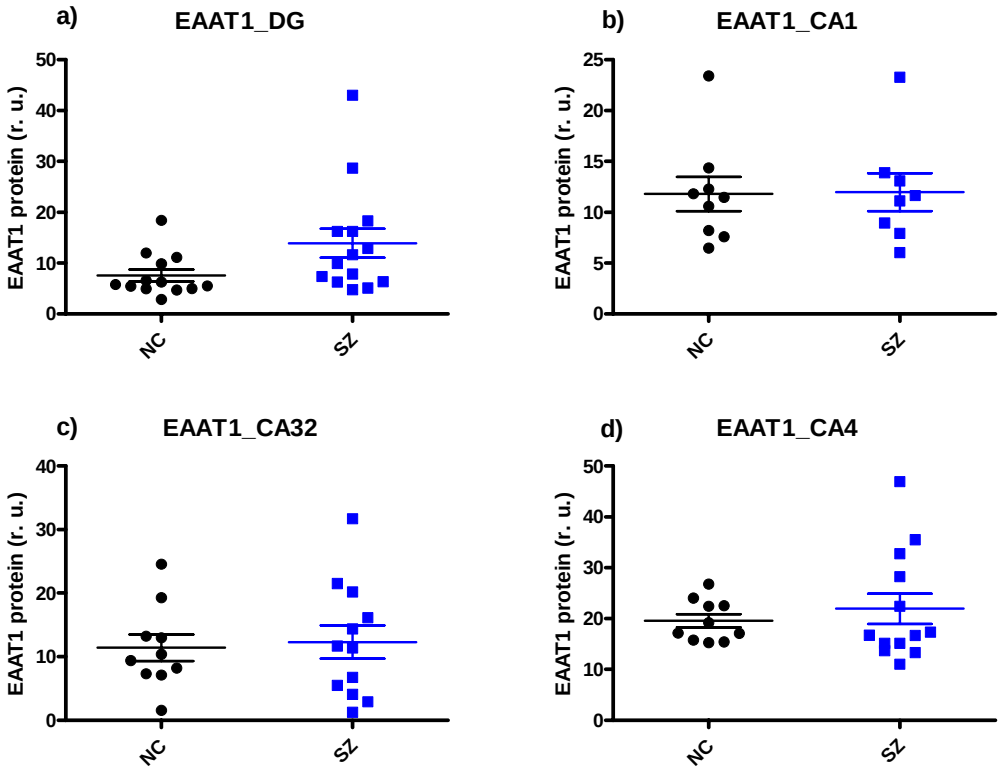

Figure 4.6. EAAT 1 protein levels (normalized to VCP) in the DG (a), CA1 (b), CA32(c), CA4 (d).

EAAT2

EAAT2 mRNA

There is a significant increase in EAAT2 mRNA in schizophrenia in the DG (p=0.05) and no difference between the groups in CA1 (p = 0.36), CA32 (p=0.92), and CA4 (p = .97).

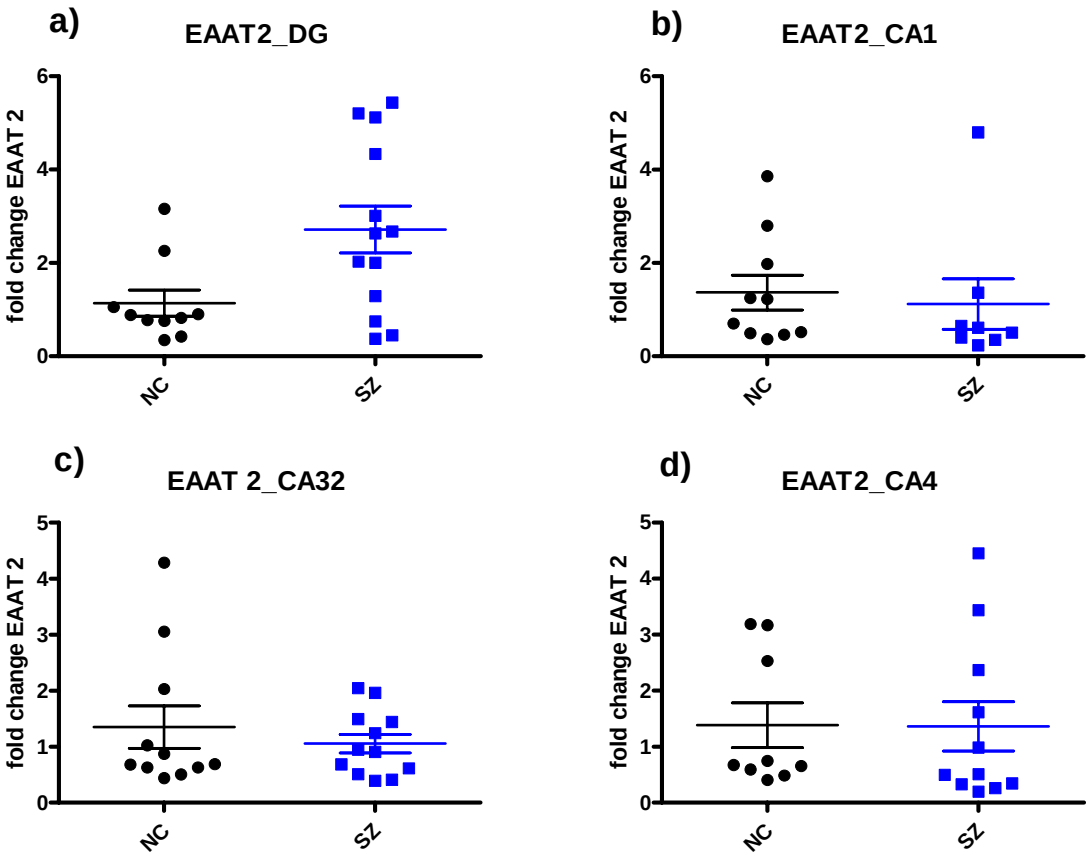

Figure 4.7. Fold changes in EAAT 2 mRNA levels in the DG (a), CA1 (b), CA32 (c), CA4 (d).

EAAT 2 Protein

There is no significant change in EAAT2 protein levels in any of the studied regions. (p = .06 DG; p = .20 CA1; p = 0.12 CA32; p = .45 CA4), although the DG difference is expressed at a trend level.

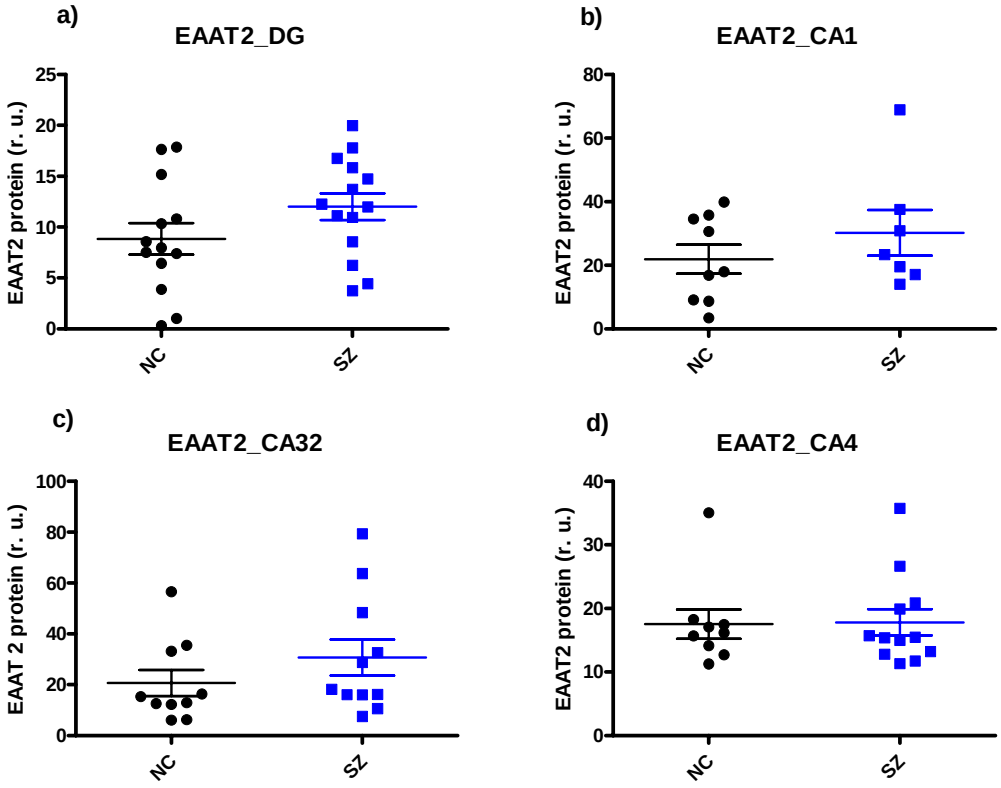

Figure 4.8. EAAT 2 protein levels (normalized to VCP) in the DG (a), CA1 (b), CA32 (c), CA4 (d).

GlyT 1

GlyT 1 mRNA

There is a trend for an increase in GlyT1 mRNA in schizophrenia in the DG (p=0.07). There is no difference between the groups in CA1 (p = 0.83), CA32 (p=0.22), and CA4 (p = .28).

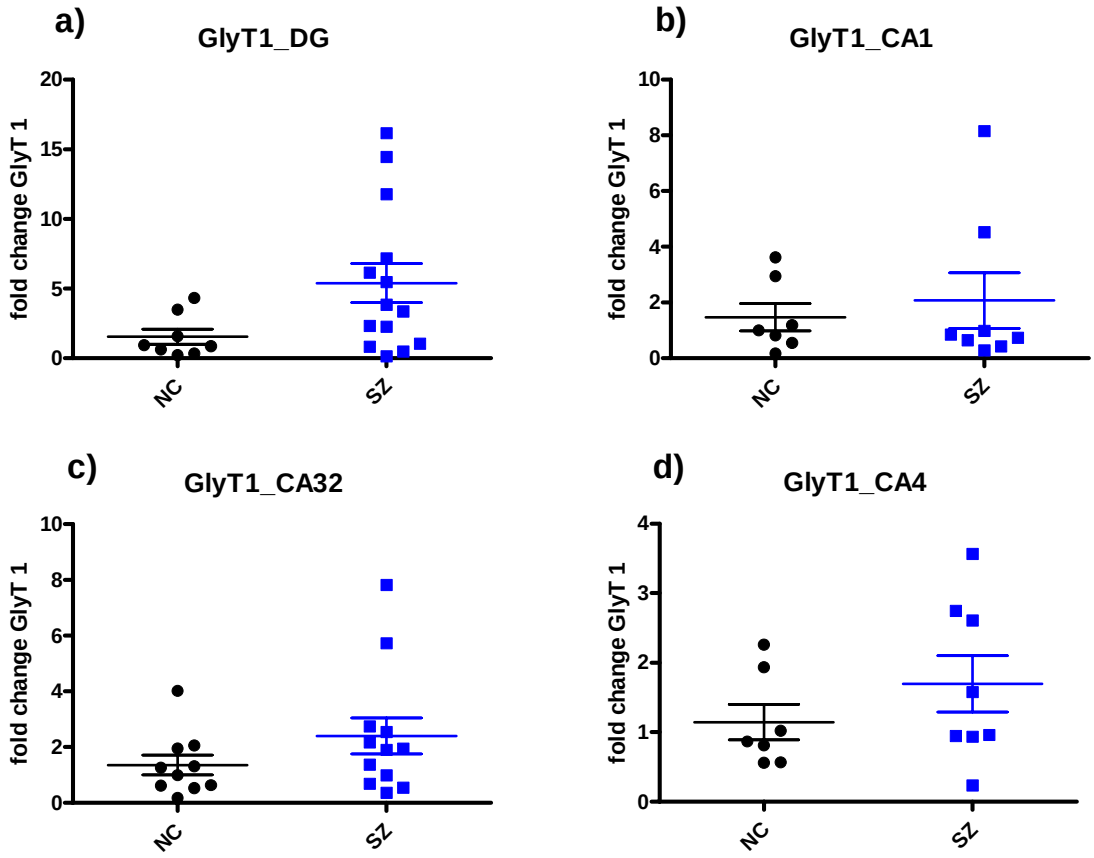

Figure 4.9. Fold changes in GlyT1 mRNA levels in the DG (a), CA1 (b), CA32 (c), CA4 (d).

No antipsychotic drug effect

As the brain tissue used in our study came from schizophrenia subjects who were typically medicated for about one third of their life, we controlled for the effect of the antipsychotic treatment on the astrocytic markers by treating four groups of rats with haloperidol, risperidone, olanzapine, and drug-free water, respectively, for 20 weeks and averaging the levels of our molecules of interest in the whole temporal lobe. For each studied drug, there no differences in the levels of GS, SR, EAAT1, EAAT2, between the control group and the drug group. (For glutamine synthetase, $p = 0.15$ for olanzapine, $p = 0.29$ for risperidone, and $p = 0.1$ for haloperidol; for serine racemase, $p = 0.79$ for olanzapine, $p = 0.77$ for risperidone, and $p = 0.62$ for haloperidol; for EAAT1, $p = 0.38$ for olanzapine, $p = 0.84$ for risperidone, and $p = 0.46$ for haloperidol; for EAAT2, $p = 0.24$ for olanzapine, $p = 0.08$ for risperidone, and $p = 0.26$ for haloperidol).

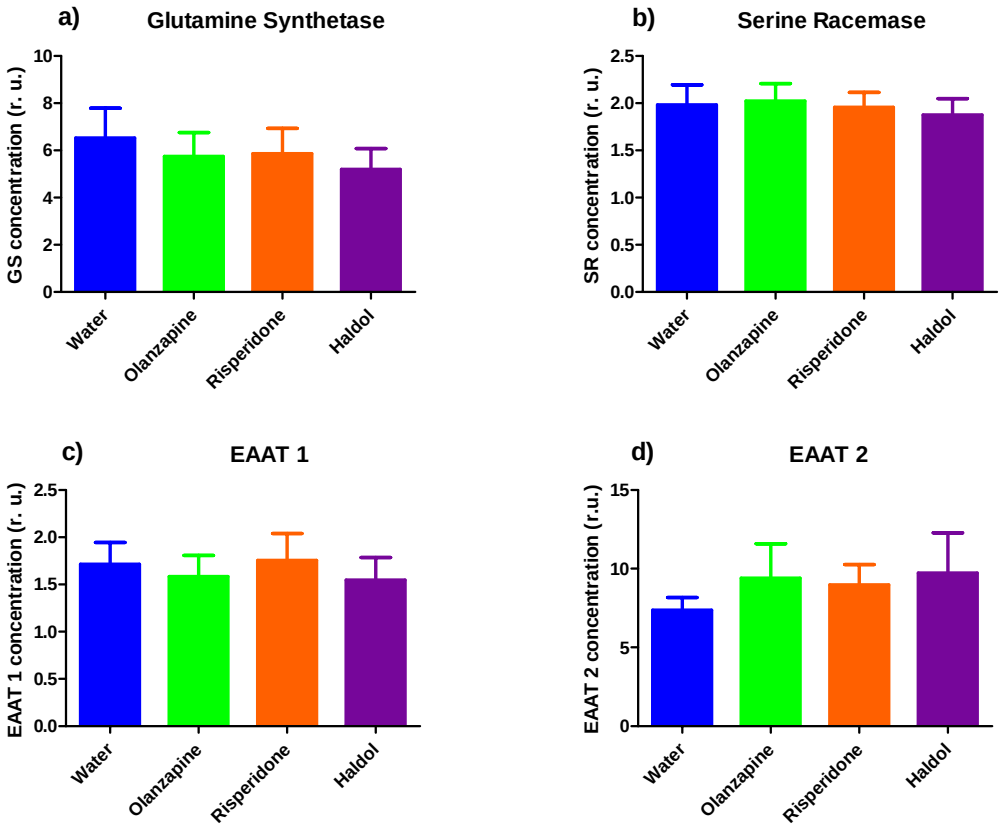

Figure 4.10. No effect of antipsychotic drug treatment (APD) on the GS protein level (a), SR protein level (b), EAAT 1protein level (c), EAAT 2 protein level (d).

Astrocyte number and density are similar in schizophrenia and control subjects

To explore whether the number and density of the astrocyte population contributed to the observed changes in the astroycte related parameters, we counted the number and density of the astrocytes in postmortem hippocampus derived from the same cohort of subjects. We found no differences between normal and schizophrenia subjects in any of the hippocampal subfields in either

astrocyte number (p = .42 DG; p = .19 CA1; p = .8 CA32; p = .93 CA4) or density (p = .78 DG; p = .22 CA1; p = .25 CA32; p = .43 CA4).

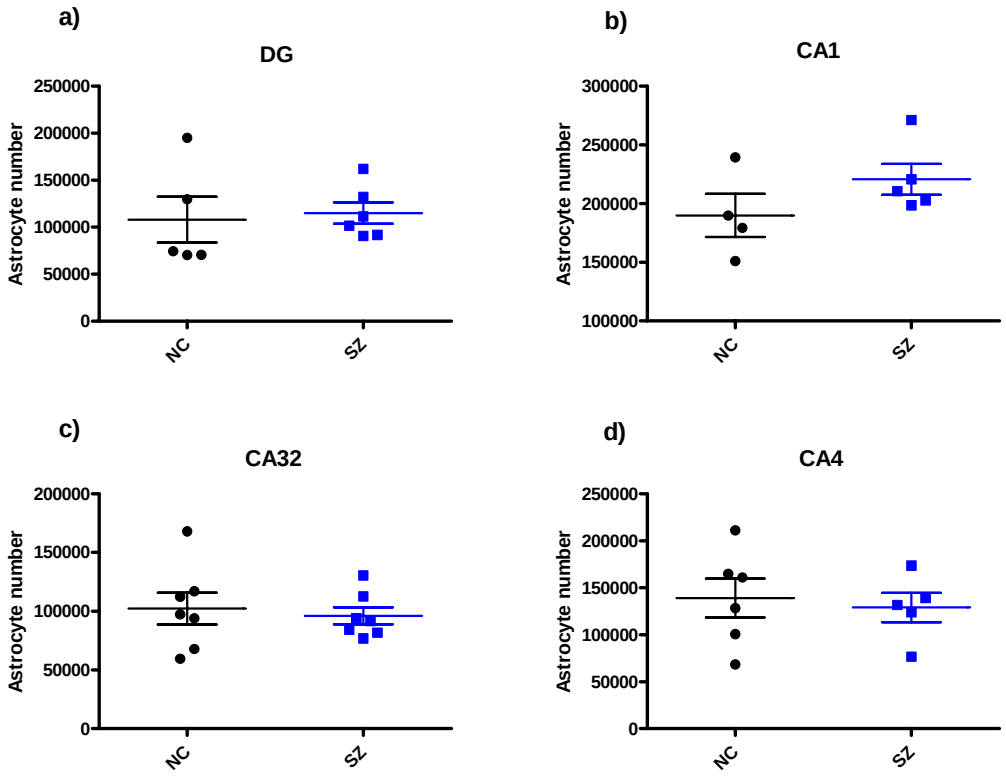

Figure 4.11. Astrocyte number in DG (a), CA1 (b), CA32 (c), and CA4 (d).

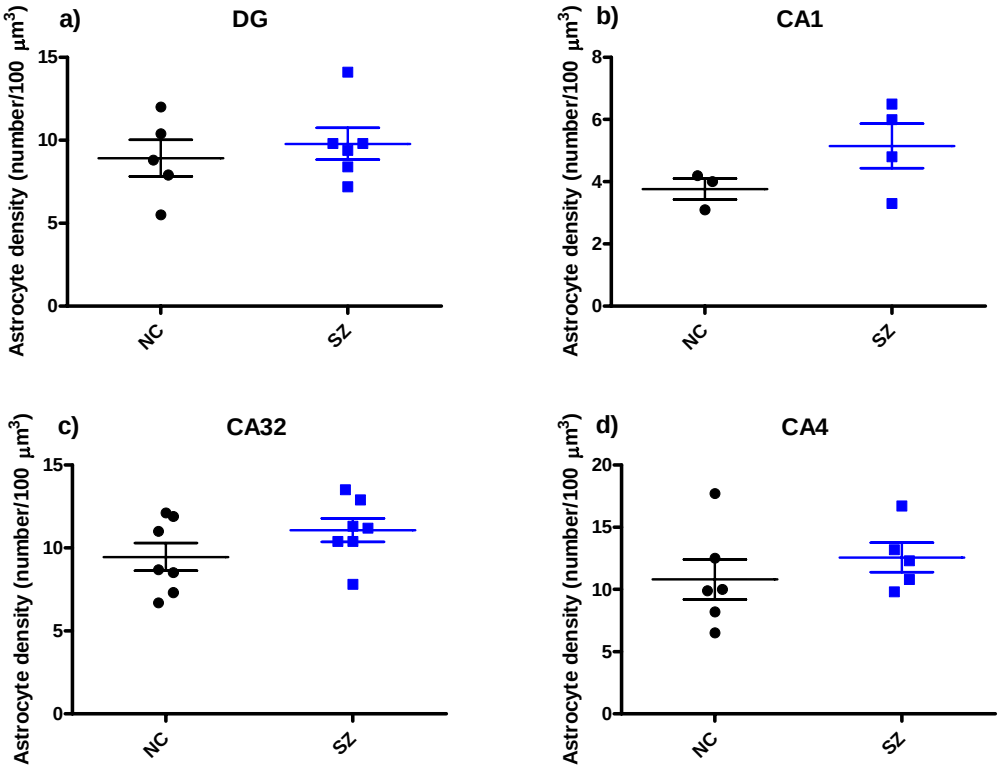

Figure 4.12. Astrocyte density in DG (a), CA1 (b), CA32 (c), and CA4 (d).

Discussion

Amongst the studied astrocyte markers, we demonstrated a significant increase of EAAT1 protein and EAAT2 mRNA in schizophrenia, accompanied by a trend level increase in EAAT2 protein and GlyT 1 mRNA. No changes were found in the protein or mRNA for GS and SR. Of note, all the detected differences are localized in the DG, pointing to areas of selective pathology in hippocampus in schizophrenia, an idea that will be revisited below.

Table 4.3. Overview of the astrocyte marker regulation in schizophrenia

Marker	mRNA	Protein
Glutamine synthetase (GS)	↔	↔
Serine racemase (SR)	↔	↔
EAAT 1	↔	↑
EAAT 2	↑	↑ (at the trend level) p = 0.06
GlyT 1	↑ (at the trend level) p = 0.07	N/A

GS protein or mRNA showed no alteration in the hippocampus in schizophrenia, a result that is consistent with the previously published reports (Steffek et al., 2008). Similarly, according to our results, levels of SR protein or mRNA did not appear to be altered in any of the hippocampal subfields in schizophrenia, although the previous two studies that examined the SR protein level in the whole hippocampus reported discordant

results: one, an increase (Steffek et al., 2006) and the other, a decrease (Bendikov et al., 2007) in the schizophrenia subjects. Most likely, the difference arises from the quality of the postmortem tissue, although this is our speculative interpretation.

With respect to the glutamate transporters, we detected an increase in EAAT1 protein that is not accompanied by a transcript increase and an increase in both EAAT2 transcript and protein. Unsurprisingly, the existent literature reports heterogenous findings of excitatory aminoacids in schizophrenia, both with respect to the brain localization and the directionality of change. For example, EAAT1 and EAAT2 transcript levels have been found to be similar in schizophrenia and normal subjects in the striatum, prefrontal cortex, and primary visual cortex (Lauriat et al., 2006; McCullumsmith and Meador-Woodruff, 2002), but increased in the thalamus (Smith et al., 2001). In the prefrontal cortex, EAAT 1 protein expression has been shown to be decreased and EAAT2 protein to be unchanged (Bauer et al., 2008).

In our sample we noted a disparity between EAAT 1 protein level, which was upregulated in schizophrenia, and the correspondent transcript, which did not change. We suspect that this is due to a more unstable EAAT1 mRNA pool in schizophrenia that contains certain alternative transcript splicing variants (Lee and Pow, 2010) that could be more susceptible to hypoxia (Sullivan et al., 2007a; Sullivan et al., 2007b). As it has recently been demonstrated, *SLC1A3*, the gene coding for the EAAT1 transporter is disrupted in some schizophrenia subjects (Walsh et al., 2008) and is thus likely to generate transcript variants that are not found in the normal subjects.

Finally, the GlyT1 transporter mRNA showed a trend to be increased in the schizophrenia tissue.

Of note, these findings are due neither to changes in the astrocyte number or density, nor to the antipsychotic treatment that schizophrenia subjects had been exposed to.

Interestingly, the differences detected in our study were all localized in the DG, where several other reports have noted a differential impairment. In particular, Reif et al (Reif et al., 2006; Reif et al., 2007) reported a reduction in KI-67, a marker of adult neurogenesis in DG in schizophrenia, suggesting that the generation of new neurons in DG may be reduced in the illness, plausibly associated with changes in the schizophrenia risk gene, DISC-1 (Duan et al., 2007) or NRG1(Barros et al., 2009; Li et al., 2007). Koolomets, Uranova, and colleagues, using electron microscopy (Kolomeets et al., 2005; Kolomeets et al., 2007), describe a reduction in the number of synapses of DG mossy fibers onto CA3 pyramidal neuronal spines in postmortem schizophrenia tissue, a finding supporting a reduction in transmission efficiency of mossy fiber synapses from DG onto CA3 neurons. In addition, NR1 mRNA—the obligate subunit of the N-methyl-d-amino (NMDA) receptor is selectively reduced within hippocampus in DG (Eastwood et al., 1995; Gao et al., 2000; Law and Deakin, 2001; Porter et al., 1997). Altar et al (Altar et al., 2005) isolated DG granule cells for microarray analysis and reported reduced gene expression coding for proteins involved in metabolism in DG. Along with findings of other molecular changes in DG in schizophrenia (Knable et al., 2004; Lauer et al., 2003), these observations indicate an emerging role for DG as a prominent hippocampal site of unique molecular pathology.

Our results are consistent with increased glutamatergic reuptake in the DG in schizophrenia, as inferred from the upregulation of the glutamatergic transporters.

Several scenarios can account for this finding:

1) A unifying lesion of the glutamatergic synapse, most likely involving the NMDA receptor, determines a compensatory increase in the synaptic glutamate and a resultant overexpression of the EAAT1 and EAAT2 transporters. The NMDA receptor hypofunction also causes a compensatory need for the co-agonist Glycine and potential overexpression of the Glycine transporter. The additional functional demand is likely handled by GS and SR with an increase in enzyme activity, rather by an overexpression of their levels.

2) One could also hypothesize that the primary lesion is an increase in the glutamate transporters, thus directly determining increased glutamate reuptake and reduced glutamate in the synapse. Low synaptic glutamate would most likely cause a compensatory upregulation of the NMDA receptor subunits. However, this is not supported by the existent schizophrenia literature, which, in contrast, documents a reduction of the obligatory NR1 subunit of the NMDA receptor. (Eastwood et al., 1995; Gao et al., 2000; Law and Deakin, 2001)

3) An alternative speculation involves the complexity of the glutamatergic synapse: each schizophrenia subject has one or two "hits", i.e., areas of primary pathology that cannot be compensated for by the remaining components of the glutamatergic synaptic system thus resulting in a hypofunctional synapse. This view is supported by a recent genome-wide analysis that identified rare structural genetic variants contributing to schizophrenia (Walsh et al., 2008), wherein genetic

mutations are overrepresented in pathways involved in brain development, including glutamatergic receptor signaling

Chapter 5

Magnetic Resonance Spectroscopy of the Medial Temporal Lobe in Schizophrenia

Introduction

Magnetic resonance spectroscopy (MRS) offers the advantage of the noninvasive measurement of neurochemical compounds *in vivo* in the human brain. It uses the same hardware as employed in fMRI BOLD imaging, albeit distinct pulse sequences to create a spectral signal. The type of output is also different: while MRI provides structural and functional information, MRS generates a neurochemical spectrum that allows the quantification of selective metabolites within a defined brain volume (Lauterbur, 1986, 2004; Ross and Michaelis, 1994).

The biophysical basis of the MRS signal is the NMR phenomenon, which occurs whenever nuclei from selected atoms are immersed in a static magnetic field and induced by the application of a second magnetic field that oscillates at the resonant frequency of the nuclei. Not all nuclei can be used to generate an MR signal; only nuclei that possess a property called spin experience the MR phenomenon. Spin is an intrinsic property of the matter conferred by the uneven distribution of electrical charge or the atomic mass. Out of all nuclei with spin, e. g. 1H, 13C, 31P, 15N, the most sensitive and abundant is 1H, making 1H MRS largely used in clinical and research applications (Patel et al., 2003; Rothman et al., 2003).

MRS is an attractive and powerful tool due to its ability to sample living human brain noninvasively, regionally and dynamically (Luyten et al., 1991). However, its

relatively poor spatial discrimination make observations at the level of cellular organization (Ross and Michaelis, 1994) a challenge when examining the subtle alterations in psychiatric disorders. Nonetheless, the MRS has been used experimentally to investigate the psychiatric pathophysiology, especially in association with other translational neuroscience methodologies, as we will do here.

We chose a focus on MRS metabolites in humans that are informative about glutamate transmission; this is based on our goal to examine the glutamatergic dysfunction in schizophrenia in the hippocampal formation, one of the brain regions involved in the manifestations of the disease (described in Chapter 1). High quality methods exist for measuring N-acetyl aspartate (NAA), glutamate, glutamine and GABA.

N-acetyl aspartate (NAA). One of the most abundant cerebral metabolites that can be the reliably detected is NAA (Moffett et al., 2007), which has been long hypothesized to be a marker of neuronal health and viability. Earlier studies associated a decrease in NAA with neuronal loss, however new evidence suggests that regional NAA reduction may be due to reversible neuronal dysfunction. The proposed roles for NAA include a) "molecular water pump" that clears the metabolic water from the neurons; b) precursor in the synthesis of the neuromodulator *N*-acetylaspartylglutamate (NAAG); c) source of the acetate moiety for postnatal myelin synthesis; d) role in energy metabolism in neuronal mitochondria (Baslow, 2003). Most published studies investigating NAA levels in schizophrenia by MRS have reported a regional decrease of approximately 5 - 10% in several brain regions, including the hippocampus, prefrontal lobe, basal ganglia, thalamus, and the anterior cingulated; however the most well - replicated and robust

findings of NAA reduction are in hippocampus and prefrontal cortex (Steen et al., 2005). An alteration in NAA in a disease group lacks specificity with respect to the type of cellular pathology present, since other brain conditions including mood disorders, tumors, stroke, multiple sclerosis, and dementia have been associated with NAA decreases (Moffett et al., 2007; Steen et al., 2005). Nonetheless, it provides some clue regarding the localization of brain areas affected in schizophrenia. Indeed, the most substantial evidence for a decrease in NAA exists in hippocampus and prefrontal cortex, where the evidence for a volume reduction, yet without a decrease in neuronal number, is also consistent.

Glutamate and glutamine. Several observations characterizing the hippocampal blood flow in schizophrenia have been made by functional magnetic resonance imaging (fMRI): a) regional cerebral blood flow (rCBF) is elevated, especially anteriorly; b) the magnitude of rCBF alteration correlates with the level of psychosis; c) the elevated rCBF is partially reduced by antipsychotic drugs (APDs).

Available evidence suggests that in the hippocampus, which is a highly excitatory organ, the local blood flow is controlled by signaling processes mediated by glutamate and modulated by GABA (Attwell and Iadecola, 2002). It is thus intriguing to speculate that the increased rCBF in the hippocampus of living schizophrenia subjects is accompanied by a change in glutamate and/or GABA concentration.

The deep off-center hippocampal positioning in the brain, as well as the field inhomogeneity surrounding the hippocampal tissue pose technical challenges in probing

the hippocampus for neurochemical data; consequently, few studies have examined hippocampal glutamate and glutamine concentrations using MRS.

The results of the one study that has reported increased glutamate concentration in schizophrenia in the left hippocampus (van Elst et al., 2005) have been questioned by the scientific community in regards to the accuracy of the metabolite concentrations presented (Theberge et al., 2007a) . More recently, a 3T study comparing hippocampal glutamate concentrations in patients with schizophrenia, their unaffected twins, and normal controls found no difference between the three groups analyzed (Lutkenhoff et al., 2008).

As other brain regions that show abnormalities in schizophrenia, including the thalamus, prefrontal cortex, and the anterior cingulate are more amenable to being probed by MRS, more reports have focused on measuring glutamate and glutamine concentrations in these areas. A transient increase in glutamine has been reported in the anterior cingulate upon ketamine administration to healthy subjects (Rowland et al., 2005), suggesting that an acute blockade of the NMDA receptor results in an upsurge of glutamatergic activity in the anterior cingulate. Increased baseline levels of glutamine, but not glutamate have been found in the anterior cingulate and the thalamus of medication naïve subjects with schizophrenia at their first psychotic break, indicating that hyperglutamatergia in the anterior cingulate and the thalamus is intrinsic to the illness pathophysiology, rather than a consequence of disease chronicity or an effect of medication administration (Theberge et al., 2002). Interestingly, the same group reported decreased levels of glutamate and glutamine in the anterior cingulate, but elevated glutamine concentration in the thalamus in chronic schizophrenia subjects, possibly due

to disease progression or medication effects (Theberge et al., 2003). More recently, glutamate has been shown to be lower in the prefrontal cortex of subjects with schizophrenia and their disease-free identical twins than in healthy controls, but no difference in glutamate concentration could be demonstrated in other sampled studied brain regions (Lutkenhoff et al., 2008). Two reports that examined the anterior cingulate cortex (ACC) as region of interest reported non-convergent results. One study was conducted on a 3T magnet (Tayoshi et al., 2009) and found decreased glutamate, but not glutamine concentrations in subjects with schizophrenia in comparison to the normal controls. The second study was performed on a 4T magnet and evaluated (NAA), Glutamate and Glutamine concentration, and Glu/Gln ratio in the anterior cingulate of subjects with recent onset schizophrenia before and after a one year course of standardized antipsychotic treatment (Bustillo et al., 2009). The subjects with recent onset schizophrenia had (lower NAA) and higher Gln/Glu than normal control subjects before the treatment. Even more, these differences maintained even after the completion of the antipsychotic course, disproving the effect of medication on the studied brain metabolites.

As described above, the results of the existent studies point to a hyperglutamatergic state at the onset of the illness, followed by a normalization/decrease of glutamatergic signal as the disease progresses, reflecting either the plastic brain changes associated with the chronic pathological process or possibly a medication effect. However, the results are often inconsistent amongst brain regions and, more importantly, the hippocampus has been rarely sampled at higher spectral fields. Therefore, our efforts

concentrated on the characterization of the hippocampal neurochemical profile in schizophrenia.

GABA. Due to low concentration and spectral overlap, GABA concentration has been studied less in schizophrenia. Goto et al. examined GABA concentrations in the frontal lobe, parieto-occipital lobe , and left basal ganglia and demonstrated a selective decrease in GABA in the left basal ganglia of subjects with the disease; no GABA measures were reported in the hippocampus (Goto et al., 2009). Recently, Tayoshi et al. found no difference in the GABA concentrations in the anterior cingulate cortex or the basal ganglia between chronic schizophrenia subjects and normal volunteers (Tayoshi et al., 2010).

Materials and Methods

Research participants

Fourteen volunteers with DSM-IV TR diagnosis of either schizophrenia or schizoaffective disorder and fourteen volunteers who neither had a history of psychiatric disease nor endorsed having first degree relatives with a psychiatric history were recruited from the Dallas metropolitan area and enrolled in this study. Inclusion criteria for all subjects comprised the following: English language fluency, competence to give informed consent, between 18 and 60 years of age, and any race or ethnicity. Exclusion criteria for all volunteers consisted of: pregnancy, breast feeding, diagnosis of an organic brain disease, significant medical illness, history of head trauma, and current use or extensive history of illicit substance use. With regard to drug use, current status was assessed via urine toxicology screen upon enrollment and, if needed, thereafter. Healthy volunteers were confirmed as free from any DSM-IV TR Axis I or II disorder, and all volunteers who were active users of neurostimulant drugs, except nicotine and caffeine, were excluded as well.

Informed consent was obtained for all participants in accordance with procedures approved by the UTSW Institutional Review Board. After giving their informed consent, the subjects underwent a brief enrollment interview followed by a more thorough diagnostic workup that included a psychiatric history, the Structured Clinical Interview for DSM-IV-TR Axis I Disorders (SCID), a urine toxicology screen, the Structured Clinical Interview for the Positive and Negative Syndrome Scale (SCI-PANSS or PANSS) (Kay et al., 1987) and the Social Functioning Scale (SFS) (Birchwood et al.,

1990). Ratings for psychosis (i.e., PANSS positive subtotals) and other symptoms were obtained by three trained research coordinators whose inter-rater reliability was r=0.84, intraclass correlation.

For final group placement, all patient volunteers met inclusive DSM-IV TR criteria for schizoaffective disorder or schizophrenia, as confirmed by diagnostic consensus between two research psychiatrists. Healthy volunteers were assessed using both the SCID and also by undergoing the Structured Interview for DSM-IV Personality (SID-P).

No changes were made to the patients' treatment regimes as part of the study, though their medication status was continually monitored. Off-medication status was assigned to SZ volunteers who had elected not to take their medication (4/14) and endorsed being APD-free for at least six weeks prior to the day of scanning.

MRS methods

Experiments were carried out on a whole-body Philips 3T scanner (Philips Medical Systems). A standarstanadd birdcage head RF coil was used for transmission and signal reception. MP-RAGE (*m*agnetization *p*repared *ra*pid *g*radient *e*cho) images were used for voxel positioning (Mugler and Brookeman, 1990). FID (free induction decay) signals were acquired in 32 blocks, each with 16 averages. Data acquisition parameters included; repetition time (TR) = 2 s, sweep width = 2.5 kHz, and number of sampling points = 2048. Shimming of the magnetic field (B_0) was achieved up to second order using the FASTMAP method. The multi-block data were corrected individually for field drift using the NAA singlet during the post-acquisition processing. LC Model software

was used for spectral fitting of the data. Quantum-mechanically calculated spectra of metabolites were used as basis functions.

Data was collected from a single voxel of 50x15x15 mm that was placed over the left hippocampus as shown in **Figure 5.1**.

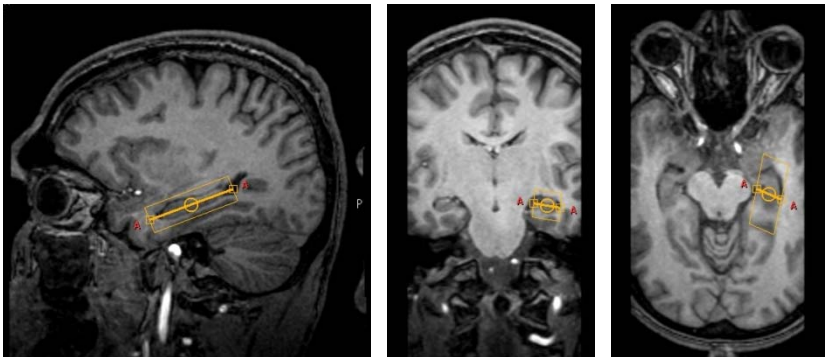

Figure 5.1. Voxel placement over the left hippocampus shown in the sagittal plane (left image), coronal plane (middle image), and transversal plane (right image).

Triple refocusing with an echo time of TE = 115 ms was used for Gln-Glu measure, which was designed for spectral discrimination between Glu and Gln at 3T. A 180° pulse that refocused resonances between 1.7 and 3.3 ppm was applied within PRESS (*p*oint-*res*olved *s*pectroscopy), thereby giving signals between 1.8 and 3.2 ppm. The Glu peak at ~2.35 ppm was somewhat suppressed to enhance the selectivity of the neighboring Gln signal. **(Fig 5.2)**

GABA was measured using scalar difference editing (MEGA) (Mescher et al., 1998). Two 15-ms Gaussian 180° pulses were implemented symmetrically about the second 180° pulse of PRESS. These Gaussian pulses, tuned to 1.89 ppm, were switched on and off in alternate scans, giving rise to a GABA edited doublet at 3.0 ppm in the

difference spectra. PRESS data were acquired as part of the MEGA editing scheme, giving a Cr signal that was used as a reference for GABA estimation. **(Fig 5.3 a and b)**

All reported values were normalized to creatine.

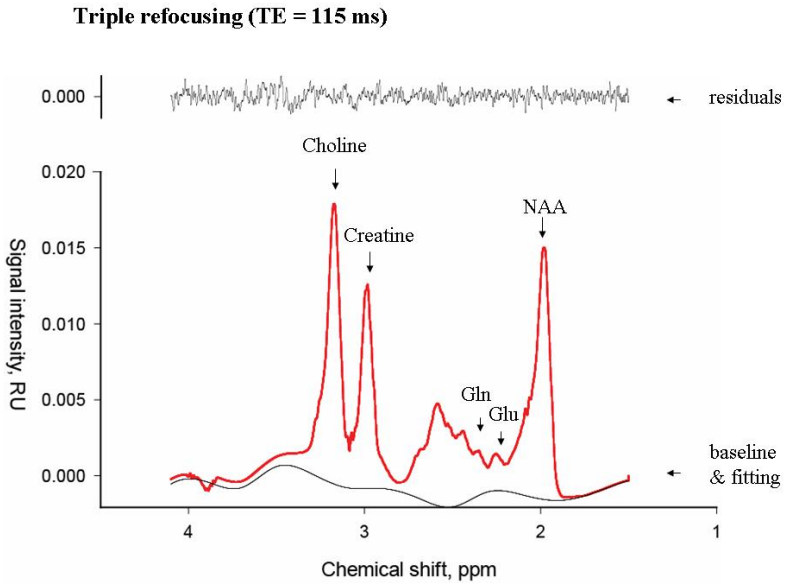

Figure 5.2. Typical triple refocusing spectrum (TE = 115) obtained at 3T from a subject with SZ. The peaks of interest are glutamate (Glu), glutamine (Gln), N-acetyl-aspartate (NAA), and Creatine.

Table 5.1. Typical data output table showing the absolute concentration of the metabolite (Conc), the standard deviation (%SD), metabolite concentration normalized to creatine (/Cr), and the metabolite abbreviation.

Conc	%SD	/Cr	Metabolite
0.137	3%	1.000	Cr
0.187	8%	1.365	Glu
3.69E-02	20%	0.269	Gln
4.51E-02	19%	0.330	Asp
0.137	3%	1.002	fCho
0.175	3%	1.281	NAA
0.247	5%	1.807	NAAasp

0.185	**3%**	**1.351**	**NAA+NAAG**
0.224	**8%**	**1.635**	**Glu+Gln**

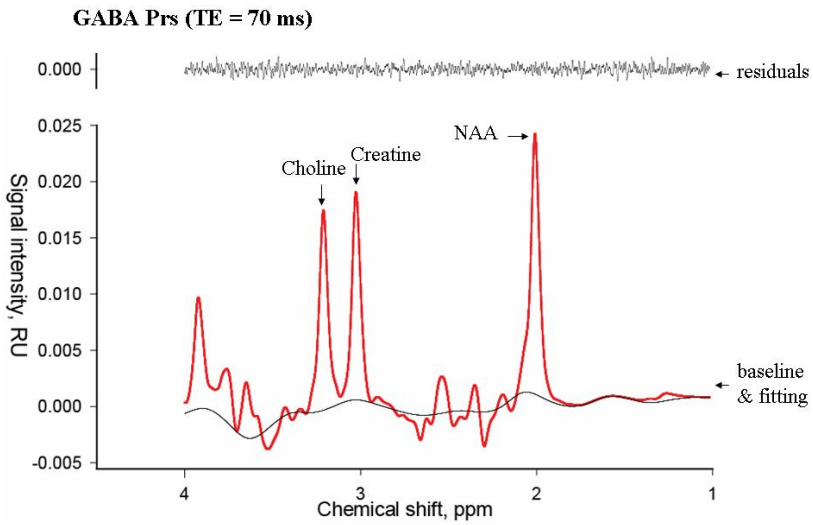

Figure 5.3a. Typical GABA point resolved spectroscopy (prs) spectrum obtained at 3T from a subject with SZ. The peak of interest is Creatine.

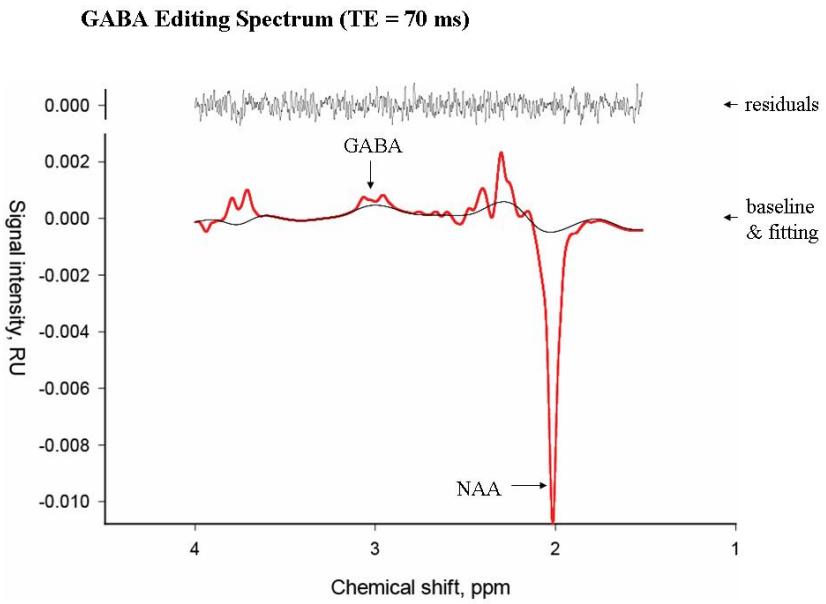

Figure 5.3b. Typical GABA editing spectrum obtained at 3T from a subject with SZ. The peak of interest is the GABA doublet.

Statistical methods

Primary analyses were conducted using one-way ANOVA tests to compare spectroscopic metabolic measurements in the three groups (NC, SZ – ON, SZ – OFF). When ANOVA tests were significant, post – hoc two tailed tests were performed, with the criterion for significance set at $p \leq .05$. Separate analyses were conducted for each metabolite: NAA, glutamate, glutamine, and GABA.

Results

We have assessed glutamate, glutamine, NAA, and GABA concentrations by ^{1}H-MRS *in vivo* in a group of normal volunteers (NC) (N = 14) in comparison with a group of schizophrenia subjects (N = 14). Out of the SZ group, 10 subjects were stabilized on antipsychotic medication (SZ – ON), whereas 4 subjects were drug-free and actively psychotic at the time of the study (SZ – OFF). Additional demographic characteristics are presented in **Table 5.2** (for the volunteers with schizophrenia) and **Table 5.3** (for the healthy volunteers).

Table 5.2. Demographic characteristics of the SZ volunteers enrolled in the MRS study.

CT	**Status**	**Age**	**Sex**	**Race**	**Smoke**	**PANSS Total**	**PANSS Positive**	**PANSS Negative**	**PANSS General**	**SFS**
1	SZ-ON	52	M	AA	1.5 ppd	76	17	19	40	137
2	SZ -OFF	23	M	C	1 ppd	97	28	18	51	N/A
3	SZ -ON	59	M	AA	2 ppd	90	24	19	47	88
6	SZ -ON	35	M	AA	0.5 ppd	88	26	20	42	121
8	SZ -ON	44	M	AA	0 ppd	84	25	17	42	145
9	SZ -ON	55	F	AA	1.5 ppd	93	24	22	47	119
10	SZ -ON	45	F	H	0 ppd	80	19	21	40	133
11	SZ -OFF	42	M	AA	1 ppd	92	25	21	46	123
20	SZ -ON	50	F	AA	1.5 ppd	90	21	22	47	122

28	SZ -ON	47	M	C	1 ppd	70	17	15	38	147
31	SZ -OFF	30	M	AA	N/A	N/A	N/A	N/A	N/A	N/A
34	SZ -ON	51	F	C	1 ppd	75	16	18	41	138
35	SZ -ON	26	M	C	1 ppd	77	21	17	39	144
37	SZ -OFF	57	M	AA	1 ppd	102	25	29	48	80

Table 5.3. Demographic characteristics of the healthy volunteers enrolled in the MRS study.

CT	**Status**	**Age**	**Sex**	**Race**	**Smoke**
0	NC	37	M	C	0
5	NC	18	F	H	0
7	NC	22	F	AA	0
14	NC	28	M	C	0
15	NC	22	M	H	1pack/week
16	NC	24	M	A	0
18	NC	41	M	AA	1.5 ppd
21	NC	36	M	C	0
23	NC	38	M	C	0
25	NC	55	F	C	0
27	NC	48	F	H	0
29	NC	22	F	C	0
30	NC	23	M	AA	1 ppd

32	NC	53	F	C	0

Glutamate

The glutamate concentration was significantly different among the 3 subject groups, NV, SV-ON, and SV-OFF ($F(2, 25) = 5.654$; $p = 0.0094$). Post hoc t- tests revealed a significant decrease in glutamate concentration in the SZ – OFF in comparison with the normal volunteers (NC: 1.138 ± 0.055; SZ-OFF, 0.7498+/- 0.084; $p = 0.0036$). This difference is diminished or 'normalized' in the antipsychotic medication-treated group, making glutamate concentration in the SZ – ON group (1.228 ± 0.096) similar to the NC group ($p = 0.39$), but significantly higher than in the non-medicated schizophrenia group ($p = 0.0128$). It can thus be inferred that decreased glutamatergic activity in the hippocampus is a state specific to untreated schizophrenia and that the antipsychotic treatment normalizes the glutamate concentration **(Figure 5.4).**

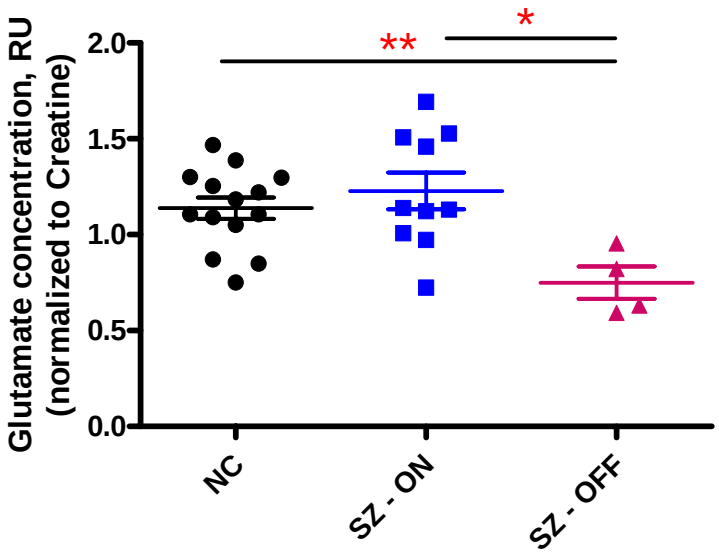

Figure 5.4. Glutamate concentrations (relative units, normalized to Creatine concentration) in the normal control group (NC; black dots), medicated schizophrenia volunteer group (SZ – ON; blue squares), and non – medicated schizophrenia volunteer group (SZ – OFF; red triangles).

Glutamine

Glutamine concentrations were similar amongst the three studied groups without any statistical evidence of change ($F(2, 25) = 0.7495$; $p = 0.482$), with the following individual values obtained: NC 0.4191 ± 0.0305; SZ – ON 0.4286 ± 0.1528; SZ – OFF 0.3400 ± 0.0871. **(Figure 5.5)**

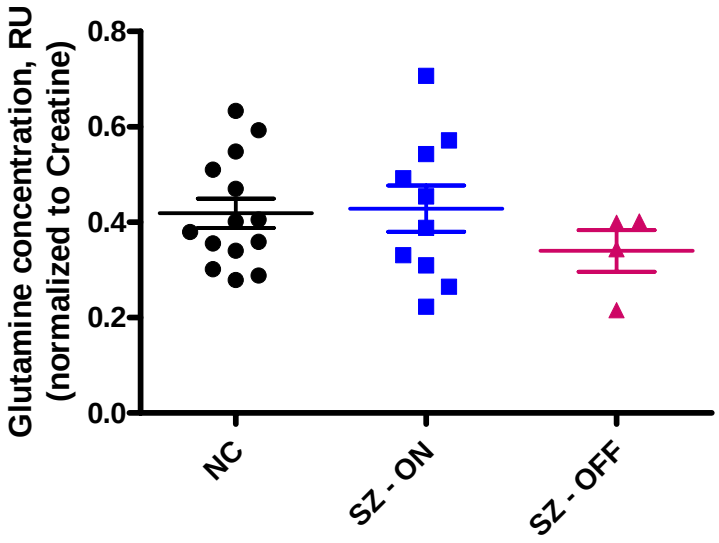

Figure 5.5. Glutamine concentrations (relative units, normalized to Creatine concentration) in the normal control group (NC; black dots), medicated schizophrenia volunteer group (SZ – ON; blue squares), and non – medicated schizophrenia volunteer group (SZ – OFF; red triangles)

NAA

There was a significant difference within the three human groups with respect to the NAA levels ($F(2, 25) = 4.509$; $p = 0.0213$), with similar values in both patient groups, with the SZ – ON (1.312 ± 0.03451) and SZ – OFF (1.353 ± 0.066) groups ($p = 0.56$). The NAA levels were observed to be significantly decreased in the SZ – ON group ($p = 0.0064$), but not in the SZ - OFF group ($p = 0.16$) compared to the NC group (1.45 ± 0.02981). (**Figure 5.6**).

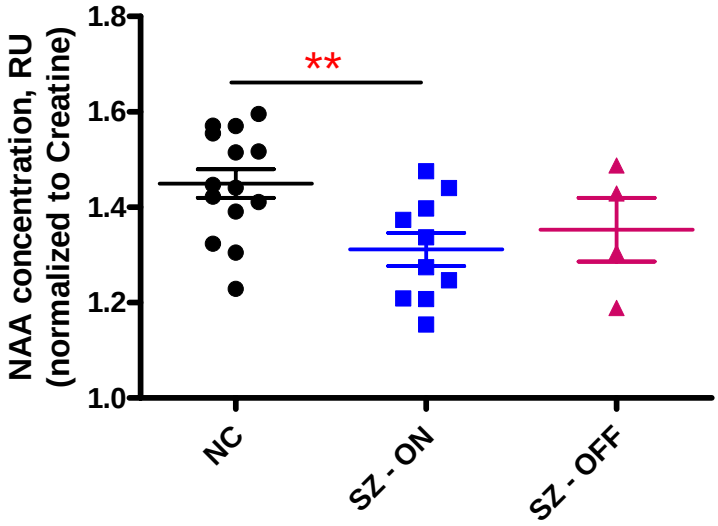

Figure 5.6. NAA concentrations (relative units, normalized to Creatine concentration) in the normal control group (NC; black dots), medicated schizophrenia volunteer group (SZ – ON; blue squares), and non – medicated schizophrenia volunteer group (SZ – OFF; red triangles)

GABA

The GABA measurements showed no significant difference amongst the three groups ($F(2, 25) = 1.533$; $p = 0.235$). The group values were as follows: NC 0.2027 ± 0.021; SZ – ON 0.2436 ± 0.0199; SZ – OFF 0.1808 ± 0.01920 (**Figure 5.7**).

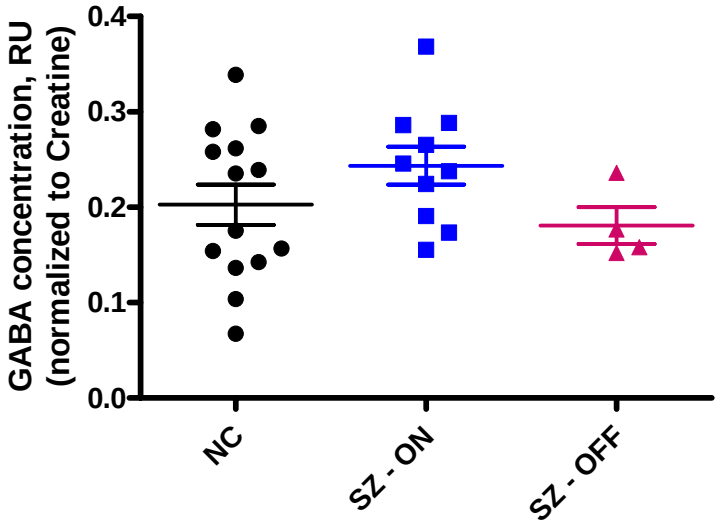

Figure 5.7. GABA concentrations (relative units, normalized to Creatine concentration) in the normal control group (NC; black dots), medicated schizophrenia volunteer group (SZ – ON; blue squares), and non – medicated schizophrenia volunteer group (SZ – OFF; red triangles)

Discussion

We have evaluated the neurochemical profile of the hippocampus with respect to the glutamatergic neurotransmission in a sample of 14 normal volunteers and 14 subjects with schizophrenia. Of the schizophrenia subjects, 10 were medicated at the time of the study and 4 were off –medication. Specifically, we measured the concentrations of 1) glutamate and glutamine, two metabolites that are directly informative of the excitatory neurotransmission; 2) GABA, the neurotransmitter that provides the inhibitory drive of the hippocampus; and 3)NAA, which indirectly influences the glutamatergic transmission.

Our findings suggest that untreated schizophrenia is associated with reduced hippocampal glutamate concentrations that are "corrected" by the antipsychotic medication, supporting the argument that hippocampal hypoglutamatergia is intrinsic to the formation of the disease and antipsychotic drug (APD) treatment has an effect of on the hippocampal glutamate. This effect is so significant that no difference in glutamate concentration is detected between the treated schizophrenia subjects and the normal controls.

This set of data is consistent with the findings of the only other undisputed study that reported glutamate concentrations in the hippocampi of probands with schizophrenia, their twins discordant for the disease, and normal controls (Lutkenhoff et al); according to their results, all three groups were found to be similar with respect to hippocampal glutamate concentrations. Unfortunately, no mention was made in regards the treatment study at the time of the scan.

The glutamate level measured by the magnetic resonance spectroscopy comprises both the neurotransmitter and the metabolic pool. The two compartments cannot be separated by this technique; however they are known to be in a linear relationship with a slope of approximately 1, suggesting that alterations in the total glutamate are likely to be reflected both in the metabolic and the neurotransmitter pool. Under this assumption, the decreased total glutamate concentration in untreated schizophrenia means that less glutamate is available for neurotransmission and, by extension, in the synaptic cleft. Thus, the decreased glutamatergic signaling in untreated schizophrenia can be explained, at least to some extent, by insufficient synaptic glutamate.

Nevertheless, the hippocampus is a multilayered, complex structure whose anatomical details are not captured by the spectroscopic measures; each hippocampal field is known to accomplish different functions (see introduction), therefore feature a particular biochemical profile. Our spectroscopic observations represent averages across all layers, but do not inform us of the diversity of the structure or the subregional differences. With this idea in mind, on overall decrease of the glutamate concentration could be the result of selective regional decreases in the context of otherwise normal concentrations in the rest of the hippocampus or, even selective regional increases superimposed on a background of decreased glutamate.

Another interesting observation derived from our study is the "correction" of hippocampal glutamate by APD treatment. No other study examined the effect of APDs on the hippocampus, therefore ours is the first demonstration that chronic treatment normalizes the neurotransmitter levels in this brain area. In regards with the other brain

regions involved in schizophrenia, the literature is equivocal with respect to medication effect, as both scenarios/possibilities have been reported: no regulation (Bustillo et al., 2006; Bustillo et al., 2009) and regulation (Arun et al., 2008; Theberge et al., 2007b) of brain metabolites by antipsychotics. Most likely, the medication effect is a function of time as well, since the long period required to achieve a visible clinical benefit is a well-known property of antipsychotics.

In our study, glutamine concentration changes did not parallel glutamate alterations. Although apparently surprising, this discordance is widely found in other reports that examined both glutamate and glutamine levels.

A reduction in NAA was noticed in the medicated schizophrenia patients as compared to the normal subjects. However, it was not observed in the off-medication schizophrenia subjects, suggesting that the NAA decrease might be the result of chronic treatment than the progression of the disease itself.

Our study is the first to examine GABA concentrations in the hippocampus in schizophrenia; no difference has been found amongst the three studied groups, suggesting no regulation of the inhibitory transmission in schizophrenia. An alternative explanation is the lack of sensitivity of the spectroscopic methods currently available for GABA measurement. Given the lower GABA concentration, the metabolite needs to be measured at a relatively short relaxation time, where macromolecule contamination is still significant.

References

Abi-Dargham, A., Rodenhiser, J., Printz, D., Zea-Ponce, Y., Gil, R., Kegeles, L.S., Weiss, R., Cooper, T.B., Mann, J.J., Van Heertum, R.L., *et al.* (2000). Increased baseline occupancy of D2 receptors by dopamine in schizophrenia. Proc Natl Acad Sci U S A *97*, 8104-8109.

Altar, C.A., Jurata, L.W., Charles, V., Lemire, A., Liu, P., Bukhman, Y., Young, T.A., Bullard, J., Yokoe, H., Webster, M.J., *et al.* (2005). Deficient hippocampal neuron expression of proteasome, ubiquitin, and mitochondrial genes in multiple schizophrenia cohorts. Biol Psychiatry *58*, 85-96.

Amara, S.G., and Fontana, A.C. (2002). Excitatory amino acid transporters: keeping up with glutamate. Neurochem Int *41*, 313-318.

Angulo, M.C., Kozlov, A.S., Charpak, S., and Audinat, E. (2004). Glutamate released from glial cells synchronizes neuronal activity in the hippocampus. J Neurosci *24*, 6920-6927.

Araque, A., Sanzgiri, R.P., Parpura, V., and Haydon, P.G. (1998). Calcium elevation in astrocytes causes an NMDA receptor-dependent increase in the frequency of miniature synaptic currents in cultured hippocampal neurons. J Neurosci *18*, 6822-6829.

Arriza, J.L., Eliasof, S., Kavanaugh, M.P., and Amara, S.G. (1997). Excitatory amino acid transporter 5, a retinal glutamate transporter coupled to a chloride conductance. Proc Natl Acad Sci U S A *94*, 4155-4160.

Arriza, J.L., Fairman, W.A., Wadiche, J.I., Murdoch, G.H., Kavanaugh, M.P., and Amara, S.G. (1994). Functional comparisons of three glutamate transporter subtypes cloned from human motor cortex. J Neurosci *14*, 5559-5569.

Arun, P., Madhavarao, C.N., Moffett, J.R., and Namboodiri, A.M. (2008). Antipsychotic drugs increase N-acetylaspartate and N-acetylaspartylglutamate in SH-SY5Y human neuroblastoma cells. J Neurochem *106*, 1669-1680.

Attwell, D., and Iadecola, C. (2002). The neural basis of functional brain imaging signals. Trends Neurosci *25*, 621-625.

Bahn, S., Augood, S.J., Ryan, M., Standaert, D.G., Starkey, M., and Emson, P.C. (2001). Gene expression profiling in the post-mortem human brain--no cause for dismay. J Chem Neuroanat *22*, 79-94.

Barrachina, M., Castano, E., and Ferrer, I. (2006). TaqMan PCR assay in the control of RNA normalization in human post-mortem brain tissue. Neurochem Int *49*, 276-284.

Barros, C.S., Calabrese, B., Chamero, P., Roberts, A.J., Korzus, E., Lloyd, K., Stowers, L., Mayford, M., Halpain, S., and Muller, U. (2009). Impaired maturation of dendritic spines without disorganization of cortical cell layers in mice lacking NRG1/ErbB signaling in the central nervous system. Proc Natl Acad Sci U S A *106*, 4507-4512.

Barton, A.J., Pearson, R.C., Najlerahim, A., and Harrison, P.J. (1993). Pre- and postmortem influences on brain RNA. J Neurochem *61*, 1-11.
Baslow, M.H. (2003). N-acetylaspartate in the vertebrate brain: metabolism and function. Neurochem Res *28*, 941-953.
Basu, A.C., Tsai, G.E., Ma, C.L., Ehmsen, J.T., Mustafa, A.K., Han, L., Jiang, Z.I., Benneyworth, M.A., Froimowitz, M.P., Lange, N., *et al.* (2009). Targeted disruption of serine racemase affects glutamatergic neurotransmission and behavior. Mol Psychiatry *14*, 719-727.
Bauer, D., Gupta, D., Harotunian, V., Meador-Woodruff, J.H., and McCullumsmith, R.E. (2008). Abnormal expression of glutamate transporter and transporter interacting molecules in prefrontal cortex in elderly patients with schizophrenia. Schizophr Res *104*, 108-120.
Bendikov, I., Nadri, C., Amar, S., Panizzutti, R., De Miranda, J., Wolosker, H., and Agam, G. (2007). A CSF and postmortem brain study of D-serine metabolic parameters in schizophrenia. Schizophr Res *90*, 41-51.
Birchwood, M., Smith, J., Cochrane, R., Wetton, S., and Copestake, S. (1990). The Social Functioning Scale. The development and validation of a new scale of social adjustment for use in family intervention programmes with schizophrenic patients. Br J Psychiatry *157*, 853-859.
Bonvento, G., Sibson, N., and Pellerin, L. (2002). Does glutamate image your thoughts? Trends Neurosci *25*, 359-364.
Braff, D.L. (1993). Information processing and attention dysfunctions in schizophrenia. Schizophr Bull *19*, 233-259.
Buesa, C., Maes, T., Subirada, F., Barrachina, M., and Ferrer, I. (2004). DNA chip technology in brain banks: confronting a degrading world. J Neuropathol Exp Neurol *63*, 1003-1014.
Bustillo, J., Barrow, R., Paz, R., Tang, J., Seraji-Bozorgzad, N., Moore, G.J., Bolognani, F., Lauriello, J., Perrone-Bizzozero, N., and Galloway, M.P. (2006). Long-term treatment of rats with haloperidol: lack of an effect on brain N-acetyl aspartate levels. Neuropsychopharmacology *31*, 751-756.
Bustillo, J.R., Rowland, L.M., Mullins, P., Jung, R., Chen, H., Qualls, C., Hammond, R., Brooks, W.M., and Lauriello, J. (2009). (1)H-MRS at 4 Tesla in minimally treated early schizophrenia. Mol Psychiatry.
Carlsson, A., Waters, N., Holm-Waters, S., Tedroff, J., Nilsson, M., and Carlsson, M.L. (2001). Interactions between monoamines, glutamate, and GABA in schizophrenia: new evidence. Annu Rev Pharmacol Toxicol *41*, 237-260.
Carpenter, W.T., Jr., and Buchanan, R.W. (1994). Schizophrenia. N Engl J Med *330*, 681-690.
Casanova, M.F., and Kleinman, J.E. (1990). The neuropathology of schizophrenia: a critical assessment of research methodologies. Biol Psychiatry *27*, 353-362.

Castensson, A., Emilsson, L., Preece, P., and Jazin, E.E. (2000). High-resolution quantification of specific mRNA levels in human brain autopsies and biopsies. Genome Res *10*, 1219-1229.
Charles, A.C., Merrill, J.E., Dirksen, E.R., and Sanderson, M.J. (1991). Intercellular signaling in glial cells: calcium waves and oscillations in response to mechanical stimulation and glutamate. Neuron *6*, 983-992.
Chaudhry, F.A., Lehre, K.P., van Lookeren Campagne, M., Ottersen, O.P., Danbolt, N.C., and Storm-Mathisen, J. (1995). Glutamate transporters in glial plasma membranes: highly differentiated localizations revealed by quantitative ultrastructural immunocytochemistry. Neuron *15*, 711-720.
Colangelo, V., Schurr, J., Ball, M.J., Pelaez, R.P., Bazan, N.G., and Lukiw, W.J. (2002). Gene expression profiling of 12633 genes in Alzheimer hippocampal CA1: transcription and neurotrophic factor down-regulation and up-regulation of apoptotic and pro-inflammatory signaling. J Neurosci Res *70*, 462-473.
Cornell-Bell, A.H., and Finkbeiner, S.M. (1991). Ca2+ waves in astrocytes. Cell Calcium *12*, 185-204.
Cornell-Bell, A.H., Finkbeiner, S.M., Cooper, M.S., and Smith, S.J. (1990). Glutamate induces calcium waves in cultured astrocytes: long-range glial signaling. Science *247*, 470-473.
Coyle, J.T. (1996). The glutamatergic dysfunction hypothesis for schizophrenia. Harv Rev Psychiatry *3*, 241-253.
Creese, I., Burt, D.R., and Snyder, S.H. (1976a). Dopamine receptor binding predicts clinical and pharmacological potencies of antischizophrenic drugs. Science *192*, 481-483.
Creese, I., Burt, D.R., and Snyder, S.H. (1976b). Dopamine receptors and average clinical doses. Science *194*, 546.
Csernansky, J.G., Wang, L., Jones, D., Rastogi-Cruz, D., Posener, J.A., Heydebrand, G., Miller, J.P., and Miller, M.I. (2002). Hippocampal deformities in schizophrenia characterized by high dimensional brain mapping. Am J Psychiatry *159*, 2000-2006.
Danbolt, N.C. (2001). Glutamate uptake. Prog Neurobiol *65*, 1-105.
Dani, J.W., and Smith, S.J. (1995). The triggering of astrocytic calcium waves by NMDA-induced neuronal activation. Ciba Found Symp *188*, 195-205; discussion 205-199.
Davis, K.L., Kahn, R.S., Ko, G., and Davidson, M. (1991). Dopamine in schizophrenia: a review and reconceptualization. Am J Psychiatry *148*, 1474-1486.
Dickinson, D., Iannone, V.N., Wilk, C.M., and Gold, J.M. (2004). General and specific cognitive deficits in schizophrenia. Biol Psychiatry *55*, 826-833.
Duan, X., Chang, J.H., Ge, S., Faulkner, R.L., Kim, J.Y., Kitabatake, Y., Liu, X.B., Yang, C.H., Jordan, J.D., Ma, D.K., *et al.* (2007). Disrupted-In-

Schizophrenia 1 regulates integration of newly generated neurons in the adult brain. Cell *130*, 1146-1158.
Duffy, S., and MacVicar, B.A. (1995). Adrenergic calcium signaling in astrocyte networks within the hippocampal slice. J Neurosci *15*, 5535-5550.
Duvernoy, H.M., and Bourgouin, P. (1998). The human hippocampus : functional anatomy, vascularization and serial sections with MRI, 2nd completely rev. and expanded edn (Berlin ; New York, Springer).
Eastwood, S.L., McDonald, B., Burnet, P.W., Beckwith, J.P., Kerwin, R.W., and Harrison, P.J. (1995). Decreased expression of mRNAs encoding non-NMDA glutamate receptors GluR1 and GluR2 in medial temporal lobe neurons in schizophrenia. Brain Res Mol Brain Res *29*, 211-223.
Eliasof, S., Arriza, J.L., Leighton, B.H., Kavanaugh, M.P., and Amara, S.G. (1998). Excitatory amino acid transporters of the salamander retina: identification, localization, and function. J Neurosci *18*, 698-712.
Fam, S.R., Gallagher, C.J., and Salter, M.W. (2000). P2Y(1) purinoceptor-mediated Ca(2+) signaling and Ca(2+) wave propagation in dorsal spinal cord astrocytes. J Neurosci *20*, 2800-2808.
Fellin, T., Pascual, O., Gobbo, S., Pozzan, T., Haydon, P.G., and Carmignoto, G. (2004). Neuronal synchrony mediated by astrocytic glutamate through activation of extrasynaptic NMDA receptors. Neuron *43*, 729-743.
Ferrer-Alcon, M., La Harpe, R., Guimon, J., and Garcia-Sevilla, J.A. (2003). Downregulation of neuronal cdk5/p35 in opioid addicts and opiate-treated rats: relation to neurofilament phosphorylation. Neuropsychopharmacology *28*, 947-955.
Furuta, A., Martin, L.J., Lin, C.L., Dykes-Hoberg, M., and Rothstein, J.D. (1997). Cellular and synaptic localization of the neuronal glutamate transporters excitatory amino acid transporter 3 and 4. Neuroscience *81*, 1031-1042.
Gao, X.M., Sakai, K., Roberts, R.C., Conley, R.R., Dean, B., and Tamminga, C.A. (2000). Ionotropic glutamate receptors and expression of N-methyl-D-aspartate receptor subunits in subregions of human hippocampus: effects of schizophrenia. Am J Psychiatry *157*, 1141-1149.
Ghose, S., Chin, R., Gallegos, A., Roberts, R., Coyle, J., and Tamminga, C. (2009). Localization of NAAG-related gene expression deficits to the anterior hippocampus in schizophrenia. Schizophr Res *111*, 131-137.
Goto, N., Yoshimura, R., Moriya, J., Kakeda, S., Ueda, N., Ikenouchi-Sugita, A., Umene-Nakano, W., Hayashi, K., Oonari, N., Korogi, Y., *et al.* (2009). Reduction of brain gamma-aminobutyric acid (GABA) concentrations in early-stage schizophrenia patients: 3T Proton MRS study. Schizophr Res *112*, 192-193.
Green, M.F., Kern, R.S., Braff, D.L., and Mintz, J. (2000). Neurocognitive deficits and functional outcome in schizophrenia: are we measuring the "right stuff"? Schizophr Bull *26*, 119-136.

Gur, R.C., Ragland, J.D., Moberg, P.J., Bilker, W.B., Kohler, C., Siegel, S.J., and Gur, R.E. (2001). Computerized neurocognitive scanning: II. The profile of schizophrenia. Neuropsychopharmacology *25*, 777-788.
Hamilton, N.B., and Attwell, D. (2010). Do astrocytes really exocytose neurotransmitters? Nat Rev Neurosci *11*, 227-238.
Harrison, P.J., Barton, A.J., Procter, A.W., Bowen, D.M., and Pearson, R.C. (1994). The effects of Alzheimer's disease, other dementias, and premortem course on beta-amyloid precursor protein messenger RNA in frontal cortex. J Neurochem *62*, 635-644.
Harrison, P.J., Heath, P.R., Eastwood, S.L., Burnet, P.W., McDonald, B., and Pearson, R.C. (1995). The relative importance of premortem acidosis and postmortem interval for human brain gene expression studies: selective mRNA vulnerability and comparison with their encoded proteins. Neurosci Lett *200*, 151-154.
Hassinger, T.D., Guthrie, P.B., Atkinson, P.B., Bennett, M.V., and Kater, S.B. (1996). An extracellular signaling component in propagation of astrocytic calcium waves. Proc Natl Acad Sci U S A *93*, 13268-13273.
Heckers, S., Rauch, S.L., Goff, D., Savage, C.R., Schacter, D.L., Fischman, A.J., and Alpert, N.M. (1998). Impaired recruitment of the hippocampus during conscious recollection in schizophrenia. Nat Neurosci *1*, 318-323.
Hegarty, J.D., Baldessarini, R.J., Tohen, M., Waternaux, C., and Oepen, G. (1994). One hundred years of schizophrenia: a meta-analysis of the outcome literature. Am J Psychiatry *151*, 1409-1416.
Heinrichs, R.W., and Zakzanis, K.K. (1998). Neurocognitive deficit in schizophrenia: a quantitative review of the evidence. Neuropsychology *12*, 426-445.
Honea, R., Crow, T.J., Passingham, D., and Mackay, C.E. (2005). Regional deficits in brain volume in schizophrenia: a meta-analysis of voxel-based morphometry studies. Am J Psychiatry *162*, 2233-2245.
Hyman, S.E., and Fenton, W.S. (2003). Medicine. What are the right targets for psychopharmacology? Science *299*, 350-351.
Hynd, M.R., Lewohl, J.M., Scott, H.L., and Dodd, P.R. (2003). Biochemical and molecular studies using human autopsy brain tissue. J Neurochem *85*, 543-562.
Imbeaud, S., Graudens, E., Boulanger, V., Barlet, X., Zaborski, P., Eveno, E., Mueller, O., Schroeder, A., and Auffray, C. (2005). Towards standardization of RNA quality assessment using user-independent classifiers of microcapillary electrophoresis traces. Nucleic Acids Res *33*, e56.
Innocenti, B., Parpura, V., and Haydon, P.G. (2000). Imaging extracellular waves of glutamate during calcium signaling in cultured astrocytes. J Neurosci *20*, 1800-1808.

Inoue, R., Hashimoto, K., Harai, T., and Mori, H. (2008). NMDA- and beta-amyloid1-42-induced neurotoxicity is attenuated in serine racemase knock-out mice. J Neurosci *28*, 14486-14491.
Insausti, R., Juottonen, K., Soininen, H., Insausti, A.M., Partanen, K., Vainio, P., Laakso, M.P., and Pitkanen, A. (1998). MR volumetric analysis of the human entorhinal, perirhinal, and temporopolar cortices. AJNR Am J Neuroradiol *19*, 659-671.
Irving, E.A., McCulloch, J., and Dewar, D. (1997). The effect of postmortem delay on the distribution of microtubule-associated proteins tau, MAP2, and MAP5 in the rat. Mol Chem Neuropathol *30*, 253-271.
Javitt, D.C., and Zukin, S.R. (1991). Recent advances in the phencyclidine model of schizophrenia. Am J Psychiatry *148*, 1301-1308.
Jones, L., Goldstein, D.R., Hughes, G.P., Strand, A., Collin, F., Dunnett, S.B., Kooperberg, C.L., Aragaki, A., Olson, J.M., Augood, S.J., *et al.* (2006). Assessment of the relationship between pre-chip and post-chip quality measures for Affymetrix GeneChip expression data. BMC Bioinformatics *7*, 211.
Kay, S.R., Fiszbein, A., and Opler, L.A. (1987). The positive and negative syndrome scale (PANSS) for schizophrenia. Schizophr Bull *13*, 261-276.
Kingsbury, A.E., Foster, O.J., Nisbet, A.P., Cairns, N., Bray, L., Eve, D.J., Lees, A.J., and Marsden, C.D. (1995). Tissue pH as an indicator of mRNA preservation in human post-mortem brain. Brain Res Mol Brain Res *28*, 311-318.
Kleckner, N.W., and Dingledine, R. (1988). Requirement for glycine in activation of NMDA-receptors expressed in Xenopus oocytes. Science *241*, 835-837.
Knable, M.B., Barci, B.M., Webster, M.J., Meador-Woodruff, J., and Torrey, E.F. (2004). Molecular abnormalities of the hippocampus in severe psychiatric illness: postmortem findings from the Stanley Neuropathology Consortium. Mol Psychiatry *9*, 609-620, 544.
Kolomeets, N.S., Orlovskaya, D.D., Rachmanova, V.I., and Uranova, N.A. (2005). Ultrastructural alterations in hippocampal mossy fiber synapses in schizophrenia: a postmortem morphometric study. Synapse *57*, 47-55.
Kolomeets, N.S., Orlovskaya, D.D., and Uranova, N.A. (2007). Decreased numerical density of CA3 hippocampal mossy fiber synapses in schizophrenia. Synapse *61*, 615-621.
Krystal, J.H., Karper, L.P., Seibyl, J.P., Freeman, G.K., Delaney, R., Bremner, J.D., Heninger, G.R., Bowers, M.B., Jr., and Charney, D.S. (1994). Subanesthetic effects of the noncompetitive NMDA antagonist, ketamine, in humans. Psychotomimetic, perceptual, cognitive, and neuroendocrine responses. Arch Gen Psychiatry *51*, 199-214.
Lahti, A.C., Holcomb, H.H., Medoff, D.R., and Tamminga, C.A. (1995a). Ketamine activates psychosis and alters limbic blood flow in schizophrenia. Neuroreport *6*, 869-872.

Lahti, A.C., Koffel, B., LaPorte, D., and Tamminga, C.A. (1995b). Subanesthetic doses of ketamine stimulate psychosis in schizophrenia. Neuropsychopharmacology *13*, 9-19.
Lahti, A.C., Weiler, M.A., Holcomb, H.H., Tamminga, C.A., Carpenter, W.T., and McMahon, R. (2006). Correlations between rCBF and symptoms in two independent cohorts of drug-free patients with schizophrenia. Neuropsychopharmacology *31*, 221-230.
Lahti, A.C., Weiler, M.A., Tamara Michaelidis, B.A., Parwani, A., and Tamminga, C.A. (2001). Effects of ketamine in normal and schizophrenic volunteers. Neuropsychopharmacology *25*, 455-467.
Lauer, M., Beckmann, H., and Senitz, D. (2003). Increased frequency of dentate granule cells with basal dendrites in the hippocampal formation of schizophrenics. Psychiatry Res *122*, 89-97.
Lauriat, T.L., Dracheva, S., Chin, B., Schmeidler, J., McInnes, L.A., and Haroutunian, V. (2006). Quantitative analysis of glutamate transporter mRNA expression in prefrontal and primary visual cortex in normal and schizophrenic brain. Neuroscience *137*, 843-851.
Lauterbur, P.C. (1986). NMR imaging in biomedicine. Cell Biophys *9*, 211-214.
Lauterbur, P.C. (2004). Nobel Lecture. All science is interdisciplinary--from magnetic moments to molecules to men. Biosci Rep *24*, 165-178.
Lavenex, P., and Amaral, D.G. (2000). Hippocampal-neocortical interaction: a hierarchy of associativity. Hippocampus *10*, 420-430.
Law, A.J., and Deakin, J.F. (2001). Asymmetrical reductions of hippocampal NMDAR1 glutamate receptor mRNA in the psychoses. Neuroreport *12*, 2971-2974.
Lee, A., and Pow, D.V. (2010). Astrocytes: Glutamate transport and alternate splicing of transporters. Int J Biochem Cell Biol.
Lee, J., Hever, A., Willhite, D., Zlotnik, A., and Hevezi, P. (2005). Effects of RNA degradation on gene expression analysis of human postmortem tissues. FASEB J *19*, 1356-1358.
Leonard, S., Logel, J., Luthman, D., Casanova, M., Kirch, D., and Freedman, R. (1993). Biological stability of mRNA isolated from human postmortem brain collections. Biol Psychiatry *33*, 456-466.
Lewis, D.A. (2002). The human brain revisited: opportunities and challenges in postmortem studies of psychiatric disorders. Neuropsychopharmacology *26*, 143-154.
Lewis, D.A., and Lieberman, J.A. (2000). Catching up on schizophrenia: natural history and neurobiology. Neuron *28*, 325-334.
Lewis, D.A., and Moghaddam, B. (2006). Cognitive dysfunction in schizophrenia: convergence of gamma-aminobutyric acid and glutamate alterations. Arch Neurol *63*, 1372-1376.

Li, B., Woo, R.S., Mei, L., and Malinow, R. (2007). The neuregulin-1 receptor erbB4 controls glutamatergic synapse maturation and plasticity. Neuron *54*, 583-597.
Li, J.Z., Vawter, M.P., Walsh, D.M., Tomita, H., Evans, S.J., Choudary, P.V., Lopez, J.F., Avelar, A., Shokoohi, V., Chung, T., *et al.* (2004). Systematic changes in gene expression in postmortem human brains associated with tissue pH and terminal medical conditions. Hum Mol Genet *13*, 609-616.
Li, X., Greenwood, A.F., Powers, R., and Jope, R.S. (1996). Effects of postmortem interval, age, and Alzheimer's disease on G-proteins in human brain. Neurobiol Aging *17*, 115-122.
Liddle, P.F., Friston, K.J., Frith, C.D., Hirsch, S.R., Jones, T., and Frackowiak, R.S. (1992). Patterns of cerebral blood flow in schizophrenia. Br J Psychiatry *160*, 179-186.
Liu, X., and Brun, A. (1995). Synaptophysin immunoreactivity is stable 36 h postmortem. Dementia *6*, 211-217.
Luby, E.D., Cohen, B.D., Rosenbaum, G., Gottlieb, J.S., and Kelley, R. (1959). Study of a new schizophrenomimetic drug; sernyl. AMA Arch Neurol Psychiatry *81*, 363-369.
Lutkenhoff, E.S., van Erp, T.G., Thomas, M.A., Therman, S., Manninen, M., Huttunen, M.O., Kaprio, J., Lonnqvist, J., O'Neill, J., and Cannon, T.D. (2008). Proton MRS in twin pairs discordant for schizophrenia. Mol Psychiatry.
Luyten, P.R., Marien, A.J., and den Hollander, J.A. (1991). Acquisition and quantitation in proton spectroscopy. NMR Biomed *4*, 64-69.
Martinez-Hernandez, A., Bell, K.P., and Norenberg, M.D. (1977). Glutamine synthetase: glial localization in brain. Science *195*, 1356-1358.
Mason, G.F., Falk Petersen, K., de Graaf, R.A., Kanamatsu, T., Otsuki, T., Shulman, G.I., and Rothman, D.L. (2003). A comparison of (13)C NMR measurements of the rates of glutamine synthesis and the tricarboxylic acid cycle during oral and intravenous administration of [1-(13)C]glucose. Brain Res Brain Res Protoc *10*, 181-190.
McCullumsmith, R.E., and Meador-Woodruff, J.H. (2002). Striatal excitatory amino acid transporter transcript expression in schizophrenia, bipolar disorder, and major depressive disorder. Neuropsychopharmacology *26*, 368-375.
Medoff, D.R., Holcomb, H.H., Lahti, A.C., and Tamminga, C.A. (2001). Probing the human hippocampus using rCBF: contrasts in schizophrenia. Hippocampus *11*, 543-550.
Mescher, M., Merkle, H., Kirsch, J., Garwood, M., and Gruetter, R. (1998). Simultaneous in vivo spectral editing and water suppression. NMR Biomed *11*, 266-272.
Milton, I.D., Banner, S.J., Ince, P.G., Piggott, N.H., Fray, A.E., Thatcher, N., Horne, C.H., and Shaw, P.J. (1997). Expression of the glial glutamate transporter

EAAT2 in the human CNS: an immunohistochemical study. Brain Res Mol Brain Res *52*, 17-31.
Mirnics, K., Middleton, F.A., Lewis, D.A., and Levitt, P. (2001). Analysis of complex brain disorders with gene expression microarrays: schizophrenia as a disease of the synapse. Trends Neurosci *24*, 479-486.
Moffett, J.R., Ross, B., Arun, P., Madhavarao, C.N., and Namboodiri, A.M. (2007). N-Acetylaspartate in the CNS: from neurodiagnostics to neurobiology. Prog Neurobiol *81*, 89-131.
Mohn, A.R., Gainetdinov, R.R., Caron, M.G., and Koller, B.H. (1999). Mice with reduced NMDA receptor expression display behaviors related to schizophrenia. Cell *98*, 427-436.
Mugler, J.P., 3rd, and Brookeman, J.R. (1990). Three-dimensional magnetization-prepared rapid gradient-echo imaging (3D MP RAGE). Magn Reson Med *15*, 152-157.
Nordahl, T.E., Kusubov, N., Carter, C., Salamat, S., Cummings, A.M., O'Shora-Celaya, L., Eberling, J., Robertson, L., Huesman, R.H., Jagust, W.*, et al.* (1996). Temporal lobe metabolic differences in medication-free outpatients with schizophrenia via the PET-600. Neuropsychopharmacology *15*, 541-554.
Norenberg, M.D. (1979). Distribution of glutamine synthetase in the rat central nervous system. J Histochem Cytochem *27*, 756-762.
Norenberg, M.D., and Martinez-Hernandez, A. (1979). Fine structural localization of glutamine synthetase in astrocytes of rat brain. Brain Res *161*, 303-310.
Panenka, W.J., Khorram, B., Barr, A.M., Smith, G.N., Lang, D.J., Kopala, L.C., Vandorpe, R.A., and Honer, W.G. (2007). A longitudinal study on the effects of typical versus atypical antipsychotic drugs on hippocampal volume in schizophrenia. Schizophr Res *94*, 288-292.
Parri, H.R., Gould, T.M., and Crunelli, V. (2001). Spontaneous astrocytic Ca2+ oscillations in situ drive NMDAR-mediated neuronal excitation. Nat Neurosci *4*, 803-812.
Patel, A.B., De Graaf, R.A., Mason, G.F., Rothman, D.L., Shulman, R.G., and Behar, K.L. (2003). Coupling of glutamatergic neurotransmission and neuronal glucose oxidation over the entire range of cerebral cortex activity. Ann N Y Acad Sci *1003*, 452-453.
Porter, J.T., and McCarthy, K.D. (1996). Hippocampal astrocytes in situ respond to glutamate released from synaptic terminals. J Neurosci *16*, 5073-5081.
Porter, R.H., Eastwood, S.L., and Harrison, P.J. (1997). Distribution of kainate receptor subunit mRNAs in human hippocampus, neocortex and cerebellum, and bilateral reduction of hippocampal GluR6 and KA2 transcripts in schizophrenia. Brain Res *751*, 217-231.

Preece, P., and Cairns, N.J. (2003). Quantifying mRNA in postmortem human brain: influence of gender, age at death, postmortem interval, brain pH, agonal state and inter-lobe mRNA variance. Brain Res Mol Brain Res *118*, 60-71.
Preece, P., Virley, D.J., Costandi, M., Coombes, R., Moss, S.J., Mudge, A.W., Jazin, E., and Cairns, N.J. (2003). An optimistic view for quantifying mRNA in post-mortem human brain. Brain Res Mol Brain Res *116*, 7-16.
Reif, A., Fritzen, S., Finger, M., Strobel, A., Lauer, M., Schmitt, A., and Lesch, K.P. (2006). Neural stem cell proliferation is decreased in schizophrenia, but not in depression. Mol Psychiatry *11*, 514-522.
Reif, A., Schmitt, A., Fritzen, S., and Lesch, K.P. (2007). Neurogenesis and schizophrenia: dividing neurons in a divided mind? Eur Arch Psychiatry Clin Neurosci *257*, 290-299.
Ross, B., and Michaelis, T. (1994). Clinical applications of magnetic resonance spectroscopy. Magn Reson Q *10*, 191-247.
Ross, B.M., Knowler, J.T., and McCulloch, J. (1992). On the stability of messenger RNA and ribosomal RNA in the brains of control human subjects and patients with Alzheimer's disease. J Neurochem *58*, 1810-1819.
Rothman, D.L., Behar, K.L., Hyder, F., and Shulman, R.G. (2003). In vivo NMR studies of the glutamate neurotransmitter flux and neuroenergetics: implications for brain function. Annu Rev Physiol *65*, 401-427.
Rothstein, J.D., Dykes-Hoberg, M., Pardo, C.A., Bristol, L.A., Jin, L., Kuncl, R.W., Kanai, Y., Hediger, M.A., Wang, Y., Schielke, J.P., *et al.* (1996). Knockout of glutamate transporters reveals a major role for astroglial transport in excitotoxicity and clearance of glutamate. Neuron *16*, 675-686.
Rothstein, J.D., Martin, L., Levey, A.I., Dykes-Hoberg, M., Jin, L., Wu, D., Nash, N., and Kuncl, R.W. (1994). Localization of neuronal and glial glutamate transporters. Neuron *13*, 713-725.
Rothstein, J.D., Patel, S., Regan, M.R., Haenggeli, C., Huang, Y.H., Bergles, D.E., Jin, L., Dykes Hoberg, M., Vidensky, S., Chung, D.S., *et al.* (2005). Beta-lactam antibiotics offer neuroprotection by increasing glutamate transporter expression. Nature *433*, 73-77.
Rowland, L.M., Bustillo, J.R., Mullins, P.G., Jung, R.E., Lenroot, R., Landgraf, E., Barrow, R., Yeo, R., Lauriello, J., and Brooks, W.M. (2005). Effects of ketamine on anterior cingulate glutamate metabolism in healthy humans: a 4-T proton MRS study. Am J Psychiatry *162*, 394-396.
Saykin, A.J., Gur, R.C., Gur, R.E., Mozley, P.D., Mozley, L.H., Resnick, S.M., Kester, D.B., and Stafiniak, P. (1991). Neuropsychological function in schizophrenia. Selective impairment in memory and learning. Arch Gen Psychiatry *48*, 618-624.

Seeman, P., Chau-Wong, M., Tedesco, J., and Wong, K. (1975). Brain receptors for antipsychotic drugs and dopamine: direct binding assays. Proc Natl Acad Sci U S A *72*, 4376-4380.
Seeman, P., and Kapur, S. (2000). Schizophrenia: more dopamine, more D2 receptors. Proc Natl Acad Sci U S A *97*, 7673-7675.
Shelton, M.K., and McCarthy, K.D. (1999). Mature hippocampal astrocytes exhibit functional metabotropic and ionotropic glutamate receptors in situ. Glia *26*, 1-11.
Shelton, M.K., and McCarthy, K.D. (2000). Hippocampal astrocytes exhibit Ca2+-elevating muscarinic cholinergic and histaminergic receptors in situ. J Neurochem *74*, 555-563.
Smith, R.E., Haroutunian, V., Davis, K.L., and Meador-Woodruff, J.H. (2001). Expression of excitatory amino acid transporter transcripts in the thalamus of subjects with schizophrenia. Am J Psychiatry *158*, 1393-1399.
Steen, R.G., Hamer, R.M., and Lieberman, J.A. (2005). Measurement of brain metabolites by 1H magnetic resonance spectroscopy in patients with schizophrenia: a systematic review and meta-analysis. Neuropsychopharmacology *30*, 1949-1962.
Steen, R.G., Mull, C., McClure, R., Hamer, R.M., and Lieberman, J.A. (2006). Brain volume in first-episode schizophrenia: systematic review and meta-analysis of magnetic resonance imaging studies. Br J Psychiatry *188*, 510-518.
Steffek, A.E., Haroutunian, V., and Meador-Woodruff, J.H. (2006). Serine racemase protein expression in cortex and hippocampus in schizophrenia. Neuroreport *17*, 1181-1185.
Steffek, A.E., McCullumsmith, R.E., Haroutunian, V., and Meador-Woodruff, J.H. (2008). Cortical expression of glial fibrillary acidic protein and glutamine synthetase is decreased in schizophrenia. Schizophr Res *103*, 71-82.
Stevens, J.R. (1973). An anatomy of schizophrenia? Arch Gen Psychiatry *29*, 177-189.
Sullivan, S.M., Lee, A., Bjorkman, S.T., Miller, S.M., Sullivan, R.K., Poronnik, P., Colditz, P.B., and Pow, D.V. (2007a). Cytoskeletal anchoring of GLAST determines susceptibility to brain damage: an identified role for GFAP. J Biol Chem *282*, 29414-29423.
Sullivan, S.M., Macnab, L.T., Bjorkman, S.T., Colditz, P.B., and Pow, D.V. (2007b). GLAST1b, the exon-9 skipping form of the glutamate-aspartate transporter EAAT1 is a sensitive marker of neuronal dysfunction in the hypoxic brain. Neuroscience *149*, 434-445.
Tamminga, C.A. (1998). Schizophrenia and glutamatergic transmission. Crit Rev Neurobiol *12*, 21-36.
Tamminga, C.A., and Holcomb, H.H. (2005). Phenotype of schizophrenia: a review and formulation. Mol Psychiatry *10*, 27-39.

Tamminga, C.A., Thaker, G.K., Buchanan, R., Kirkpatrick, B., Alphs, L.D., Chase, T.N., and Carpenter, W.T. (1992). Limbic system abnormalities identified in schizophrenia using positron emission tomography with fluorodeoxyglucose and neocortical alterations with deficit syndrome. Arch Gen Psychiatry *49*, 522-530.
Tanaka, K., Watase, K., Manabe, T., Yamada, K., Watanabe, M., Takahashi, K., Iwama, H., Nishikawa, T., Ichihara, N., Kikuchi, T., *et al.* (1997). Epilepsy and exacerbation of brain injury in mice lacking the glutamate transporter GLT-1. Science *276*, 1699-1702.
Tayoshi, S., Nakataki, M., Sumitani, S., Taniguchi, K., Shibuya-Tayoshi, S., Numata, S., Iga, J., Ueno, S., Harada, M., and Ohmori, T. (2010). GABA concentration in schizophrenia patients and the effects of antipsychotic medication: a proton magnetic resonance spectroscopy study. Schizophr Res *117*, 83-91.
Tayoshi, S., Sumitani, S., Taniguchi, K., Shibuya-Tayoshi, S., Numata, S., Iga, J., Nakataki, M., Ueno, S., Harada, M., and Ohmori, T. (2009). Metabolite changes and gender differences in schizophrenia using 3-Tesla proton magnetic resonance spectroscopy (1H-MRS). Schizophr Res *108*, 69-77.
Tepest, R., Wang, L., Miller, M.I., Falkai, P., and Csernansky, J.G. (2003). Hippocampal deformities in the unaffected siblings of schizophrenia subjects. Biol Psychiatry *54*, 1234-1240.
Theberge, J., Al-Semaan, Y., Williamson, P.C., Menon, R.S., Neufeld, R.W., Rajakumar, N., Schaefer, B., Densmore, M., and Drost, D.J. (2003). Glutamate and glutamine in the anterior cingulate and thalamus of medicated patients with chronic schizophrenia and healthy comparison subjects measured with 4.0-T proton MRS. Am J Psychiatry *160*, 2231-2233.
Theberge, J., Bartha, R., Drost, D.J., Menon, R.S., Malla, A., Takhar, J., Neufeld, R.W., Rogers, J., Pavlosky, W., Schaefer, B., *et al.* (2002). Glutamate and glutamine measured with 4.0 T proton MRS in never-treated patients with schizophrenia and healthy volunteers. Am J Psychiatry *159*, 1944-1946.
Theberge, J., Jensen, J.E., and Rowland, L.M. (2007a). Regarding "Increased prefrontal and hippocampal glutamate concentration in schizophrenia: evidence from a magnetic resonance spectroscopy study". Biol Psychiatry *61*, 1218-1219; author reply 1219-1220.
Theberge, J., Williamson, K.E., Aoyama, N., Drost, D.J., Manchanda, R., Malla, A.K., Northcott, S., Menon, R.S., Neufeld, R.W., Rajakumar, N., *et al.* (2007b). Longitudinal grey-matter and glutamatergic losses in first-episode schizophrenia. Br J Psychiatry *191*, 325-334.
Tomita, H., Vawter, M.P., Walsh, D.M., Evans, S.J., Choudary, P.V., Li, J., Overman, K.M., Atz, M.E., Myers, R.M., Jones, E.G., *et al.* (2004). Effect of

agonal and postmortem factors on gene expression profile: quality control in microarray analyses of postmortem human brain. Biol Psychiatry *55*, 346-352.
Torrey, E.F., Webster, M., Knable, M., Johnston, N., and Yolken, R.H. (2000). The stanley foundation brain collection and neuropathology consortium. Schizophr Res *44*, 151-155.
Trotter, S.A., Brill, L.B., 2nd, and Bennett, J.P., Jr. (2002). Stability of gene expression in postmortem brain revealed by cDNA gene array analysis. Brain Res *942*, 120-123.
van Elst, L.T., Valerius, G., Buchert, M., Thiel, T., Rusch, N., Bubl, E., Hennig, J., Ebert, D., and Olbrich, H.M. (2005). Increased prefrontal and hippocampal glutamate concentration in schizophrenia: evidence from a magnetic resonance spectroscopy study. Biol Psychiatry *58*, 724-730.
van Os, J., and Kapur, S. (2009). Schizophrenia. Lancet *374*, 635-645.
Ventura, R., and Harris, K.M. (1999). Three-dimensional relationships between hippocampal synapses and astrocytes. J Neurosci *19*, 6897-6906.
Verkhratsky, A., and Kettenmann, H. (1996). Calcium signalling in glial cells. Trends Neurosci *19*, 346-352.
Verkhratsky, A., Orkand, R.K., and Kettenmann, H. (1998). Glial calcium: homeostasis and signaling function. Physiol Rev *78*, 99-141.
Walker, M.A., Highley, J.R., Esiri, M.M., McDonald, B., Roberts, H.C., Evans, S.P., and Crow, T.J. (2002). Estimated neuronal populations and volumes of the hippocampus and its subfields in schizophrenia. Am J Psychiatry *159*, 821-828.
Walsh, T., McClellan, J.M., McCarthy, S.E., Addington, A.M., Pierce, S.B., Cooper, G.M., Nord, A.S., Kusenda, M., Malhotra, D., Bhandari, A.*, et al.* (2008). Rare structural variants disrupt multiple genes in neurodevelopmental pathways in schizophrenia. Science *320*, 539-543.
Watase, K., Hashimoto, K., Kano, M., Yamada, K., Watanabe, M., Inoue, Y., Okuyama, S., Sakagawa, T., Ogawa, S., Kawashima, N.*, et al.* (1998). Motor discoordination and increased susceptibility to cerebellar injury in GLAST mutant mice. Eur J Neurosci *10*, 976-988.
Wolosker, H., Blackshaw, S., and Snyder, S.H. (1999). Serine racemase: a glial enzyme synthesizing D-serine to regulate glutamate-N-methyl-D-aspartate neurotransmission. Proc Natl Acad Sci U S A *96*, 13409-13414.
Xia, M., Liu, Y., Figueroa, D.J., Chiu, C.S., Wei, N., Lawlor, A.M., Lu, P., Sur, C., Koblan, K.S., and Connolly, T.M. (2004). Characterization and localization of a human serine racemase. Brain Res Mol Brain Res *125*, 96-104.